AD NUMBER

AD010768

NEW LIMITATION CHANGE

TO

Approved for public release, distribution unlimited

FROM

Distribution authorized to U.S. Gov't. agencies and their contractors; Administrative/Operational Use; SEP 1952. Other requests shall be referred to Office of Naval Research, Arlington, VA 22203.

AUTHORITY

ONR ltr dtd 9 Nov 1977

AD-

10768

UNCLASSIFIED

California Inst. of Technology
Nonr 220(03)
Sept 15

CALIFORNIA INSTITUTE OF TECHNOLOGY
GUGGENHEIM JET PROPULSION CENTER
PASADENA, CALIFORNIA

QUANTITATIVE STUDIES OF APPARENT ROTATIONAL TEMPERATURES OF OH IN EMISSION AND ABSORPTION (SPECTRAL LINES WITH DOPPLER CONTOUR)

Technical Report No. V (Revised and Extended)
Contract No. Nonr-220(03), NR 015 210
Submitted by: S. S. Penner
September 1952

QUANTITATIVE STUDIES OF APPARENT ROTATIONAL TEMPERATURES OF OH IN EMISSION AND ABSORPTION (SPECTRAL LINES WITH DOPPLER CONTOUR)*

S. S. Penner

Guggenheim Jet Propulsion Center
California Institute of Technology
Pasadena, California

Even if a Boltzmann distribution exists for the population of molecules in various energy levels, it is not possible to obtain a satisfactory interpretation of experimental data by the use of conventional procedures unless the product of maximum spectral absorption coefficient K_{max} and optical density X is sufficiently small. Detailed calculations are presented which show that the experimental results, which suggest an anomalous rotational temperature for the $^2\Sigma$ - state of OH in low-pressure combustion flames, can be accounted for by using sufficiently large values for $K_{max}X$. Conventional plots for the determination of population temperatures for an isothermal emitting system at 3000°K are summarized for the P_1- and P_2- branches of the (0,0)- band of OH for $^2\Sigma \rightarrow {}^2\Pi$ transitions. Apparent population temperatures up to 19,000°K are obtained. Particularly noteworthy is a falling off in intensity for the higher rotational energy levels, which can be seen to represent a natural consequence of the fact that the maximum spectral emissivity decreases rapidly with increasing rotational energy of the initial state. (Section II).

Representative absorption studies for the determination of rotational temperatures in isothermal systems have been analyzed for the P_1- branch, (0,0)- band, $^2\Pi \rightarrow {}^2\Sigma$ transitions of OH at 3000°K. The calculations show that erroneous interpretation of experimental results occurs if the product of maximum absorption coefficient (K_{max}) and optical density (X) is not small compared to unity. Sample calculations for a blackbody light source show that the customary procedure for treating experimental results will permit adequate correlation of the data by straight lines up to relatively large values for $K_{max}X$. It is remarkable that the preceding statement remains true even under conditions in which emission data for the $^2\Sigma \rightarrow {}^2\Pi$ transitions clearly indicate that $K_{max}X$ is no longer small compared to unity. The apparent rotational temperature of the ground electronic state varies by only a few hundred degrees when the temperature of the light source is increased from 3500°K to 8000°K, the direction of the change being such that the apparent temperatures of the absorber are the more nearly in agreement with the actual temperature of the flame the higher the temperature of the light source. The calculations emphasize the fact that correlation of experimental data by straight lines is no assurance that an error in interpretation is not being made. (Section III).

---

* Supported by the ONR under Contract Nonr-220(03), NR 015 210.

Representative calculations to determine observable peak and total intensity ratios in emission for spectral lines with Doppler contour have been carried out for $^2\Sigma \rightarrow {}^2\Pi$ transitions, (0,0)- band, P_1- branch of OH at 3000°K. The calculations show that the ratios of peak and total intensities are functions of the products of maximum absorption coefficients (P_{max}) and optical density (X) for the lines under study. Hence quantitative interpretation of experimental data is not always possible unless proper account is taken of the influence of absolute intensities on experimental results. (Section IV).

Quantitative calculations have been carried out of apparent rotational temperatures in isothermal systems containing non-equilibrium distributions of OH at 3000°K and at 6000°K. The calculations on the P_1- branch, $^2\Sigma \rightarrow {}^2\Pi$ transitions, indicate that, in the absence of self-absorption, conventional plots showing discontinuities necessarily overestimate one and underestimate the other of the known temperatures of 3000°K and 6000°K. (Section V).

Quantitative calculations on the nature of distortions produced when an isothermal region at 3000°K is viewed through an isothermal region at 1500°K show that the presence of a non-isothermal field of view magnifies the distortion produced by self-absorption alone. (Section VI).

On the basis of the non-controversial quantitative calculations described in Sections II to VI for idealized systems, some speculations regarding the significance of reported flame temperature anomalies for OH are presented in Section VII.

I. INTRODUCTION

Experimental studies of population temperatures in flames have been reported, by different investigators, for the $^2\Sigma \rightarrow {}^2\Pi$ transitions in flames at low pressures[1,2] and at atmospheric pressures.[1,3,4] When the experimental data are treated according to conventional techniques,[1,2 4] the plots which are used for the determination of rotational temperatures

---

1 A. G. Gaydon and H. G. Wolfhard, Proc. Roy. Soc. (London) A194, 169 (1948); A199, 89 (1949); A201, 561 (1950); A201, 570 (1950); A205, 118 (1951); A208, 63 (1951).

2 S. S. Penner, M. Gilbert, and D. Weber, J. Chem. Phys. 20, 522 (1952). For a detailed description of the low-pressure flame apparatus see M. Gilbert, "The Investigation of Low-Pressure Flames", Report No.4-54 (Jet Propulsion Laboratory, Pasadena, August 30, 1949).

3 H. P. Broida and K. E. Shuler, J. Chem. Phys. 20, 168 (1952).

4 H. P. Broida, J. Chem. Phys. 19, 1383 (1951).

are sometimes found to exhibit discontinuities or curvatures both in the regions of small and large values of the rotational energy E(K) of the initial (upper) state. The "discontinuities" observed for small values of K have been variously attributed to the formation of OH in the excited electronic state by different chemical reactions leading to a bimodal distribution of population densities,[1,4] to falsification of experimental data by absorption of emitted radiation by cooler gas layers through which the flame is viewed,[4] and to self-absorption.[5] The curvatures observed for large values of K have been interpreted[1] to indicate predissociation according to the process

$$OH\left(^2\Sigma^+\right) \longrightarrow OH\left(^2\Sigma^-\right) \longrightarrow O(^3P) + H(^2S).$$

In a previous publication[6] we have called attention to the fact that the best available intensity estimates[7] on OH indicate that the product of the maximum absorption coefficient P_{max} and of the optical density of the emitters X is not small compared to unity for the more intense spectral lines of OH in representative low-pressure flames. In order to obtain reliable quantitative data upon which a rational interpretation of flame spectra can be based, we shall investigate theoretically, as an essential step in the interpretation of flame spectra, the radiation characteristics of various idealized systems both in emission and in absorption.

---

5 G. H. Dieke and H. M. Crosswhite, The Ultraviolet Bands of OH, The Johns Hopkins University, Bumblebee Series Report No. 87, 1948.

6 S. S. Penner, J. Chem. Phys. 20, 507 (1952).

7 R. J. Dwyer and O. Oldenberg, J. Chem. Phys. 12, 351 (1944); O. Oldenberg and F. F. Rieke, J. Chem. Phys. 6, 439 (1938).

In Section II we examine quantitatively the effect of the size of $P_{max}X$ on apparent population temperatures in isothermal systems for emission experiments. This study leads us to the conclusion that most of the experimental data could be accounted for by a population temperature which is close to the adiabatic flame temperature. Thus, the quantitative calculations are in agreement with Dieke's remarks that the observed discontinuities or curvatures for small values of E_K may be the result of self-absorption. Furthermore, an apparent falling off in intensity for large values of E_K could also be the result, in part, of falsification of experimental data by self-absorption.

In Section III we indicate briefly possible effects of large values of $P_{max}X$ on apparent population temperatures T_ℓ obtained in absorption experiments for spectral lines with Doppler contour. The results of calculations for $^2\Pi \rightarrow {}^2\Sigma$ transitions of OH and the (C,O)- band show that the apparent population temperature is strongly dependent on the numerical value of $P_{max}X$ and relatively insensitive to the temperature of the light source, as long as the source is appreciably hotter than the flame.

In Section IV quantitative calculations are described on the influence of absolute values of spectral emissivities on the use of the isointensity methods.[5,8] Representative calculations have been carried out for $^2\Sigma^- \rightarrow {}^2\Pi$ transitions of OH at 3000°K for the (0,0)- band and the P_1- branch. The results of the present analysis show that temperature anomalies, obtained by use of the isointensity method, could be the result of failure to allow for the effect of [redacted] values of the spectral emissivity on the peak and total intensities of spectral lines with Doppler contour.

---

[8] K. E. Shuler, J. Chem. Phys. 18, 1466 (1950).

In Section V the radiation characteristics of a [redacted] non-equilibrium mixture of OH are investigated in terms of conventional and isointensity methods for the interpretation of emission experiments. These calculations show that even for [redacted] systems without self-absorption the interpretation of experimental data is not unambiguous as long as conventional plots show any deviations from linearity. Furthermore, at least for the P_1- branch, linear isointensity plots of the Shuler-type are no assurance for thermal equilibrium of the emitter.

In Section VI a simplified model is used to study the simultaneous distortion of experimental data by the combined effects of self-absorption and temperature gradients. These studies show that observation of a hot isothermal region through a cooler gas layer accentuates the distortion produced in conventional plots for the interpretation of emission data.

The material presented in Sections II to VI rests on accepted procedures for the analysis of radiating systems and spectral lines with Doppler contour. The results obtained are not applicable to real flames without conjectures. However, on the basis of the quantitative studies described in Sections II to VI, some words of caution regarding the acceptance of anomalous population temperatures for OH appear to be justified. (Section VII).

II. THE EFFECT OF SELF-ABSORPTION ON APPARENT POPULATION TEMPERATURES IN EMISSION EXPERIMENTS

The effect of instrumental distortion on experimental data will be neglected in the present discussion. For the sake of simplicity, a complete analysis will be carried out only for studies involving peak intensities. It is shown in Appendix I that the results obtained for total intensities, for representative calculations, are similar to those obtained for peak

intensities.* Hence the applicability of the principal conclusions reached in the following discussion depends only on the experimental determination of valid relative peak or integrated intensities for different spectral lines.

A. Equations for the Determination of Apparent Population Temperatures

For spectral lines with Doppler contour the maximum observable intensity in emission, I_{max}, is given by the relation

$$I_{max} = R^{o}(\nu_{\ell u}) \left[1 - \exp\left(-P_{max} X\right)\right] \tag{1}$$

where $R^{o}(\nu_{\ell u})$ denotes the intensity of radiation emitted by a blackbody, which is at the same temperature T_u as the gaseous emitters under study. The frequency $\nu_{\ell u}$ is obtained from the values of the upper (E_u) and lower (E_ℓ) energy levels by use of the Bohr frequency relation. For spectral lines with Doppler contour it is well-known that $P_{max} = S_{\ell u} (mc^2/2\pi kT_t \nu_{\ell u}^2)^{\frac{1}{2}}$, where $S_{\ell u}$ is the integrated intensity for the transition under study, m equals the mass of the radiator, c is the velocity of light, k represents the Boltzmann constant, and T_t is the translational temperature.[6] Let

$$\varepsilon' = I_{max}/R^{o}(\nu_{\ell u}) \tag{2}$$

and

$$x = - P_{max} X \tag{3}$$

whence it follows that

$$-\varepsilon' = \sum_{n=1}^{\infty} x^n/n! = \exp(x) - 1. \tag{4}$$

---

* In general, peak intensity ratios are obtained if the instrumental slit width is small compared to the line-width, whereas total intensity ratios are measured when the instrumental slit-width is large compared to the line-width.

It is evident that ε' represents the maximum value of the spectral emissivity for the emitted spectral lines.* If the population temperature of the emitter is defined in the usual way, then $\varepsilon' \leq 1$.

By using Eq. (1) and the defining relations for ε' and x it is readily shown that

$$-x = \varepsilon' \left[1 + \tfrac{1}{2}\varepsilon' + (1/3)(\varepsilon')^2 + (1/4)(\varepsilon')^3 + \cdots \right] = -\ln(1-\varepsilon'). \quad (5)$$

For very small values of ε', Eq. (5) leads to the usual result, viz, $-x = \varepsilon'$ or

$$(S_{\ell u} X)(mc^2/2\pi k T_t \nu_{\ell u})^{\frac{1}{2}} = I_{max}/R^0(\nu_{\ell u}) \text{ for } \varepsilon' \ll 1. \quad (6)$$

From an appropriate expression for $S_{\ell u}$ and Eq. (6), it is readily shown that[6]

$$\frac{\partial \ln \left[I_{max}/(\nu_{\ell u})^3 g_u (q_{\ell u})^2 \right]}{\partial E_u} = -\frac{1}{kT_u} \text{ for } \varepsilon' \ll 1 \quad (7)$$

where g_u is the statistical weight of the upper (initial) energy state and $q_{\ell u}$ is the matrix element for the transition under study.

If ε' is not small compared to unity then it is no longer possible to obtain the value of T_u in a simple manner unless numerical values of ε' are available.

B. A Method for Demonstrating the Effect of Self-Absorption on Apparent Population Temperatures of OH ($^2\Sigma \rightarrow {}^2\Pi$ Transitions).

We proceed now to examine quantitatively the effect of the values of ε' on apparent population temperatures determined according to Eq. (7).

---

* Representative values of $\varepsilon'(1)$ for low-pressure flames lie between 0.3 and 0.90. In order to utilize the data given in Table II of Ref. 6 for the calculation of $\varepsilon'(1)$ care must be taken to use for X the optical density of emitter in the ground level involved in a given transition.

Plots of $\log\left[I_{max}/(\nu_{\ell u})^3 \varepsilon_u (q_{\ell u})^2 \right]$ as a function of E_u can be constructed for various assumed values of ε' by proceeding according to the scheme outlined below.

(1) Assume a value of ε', for example, for the P_1- branch, (0,0)- band, for the transition identified by the index K = 1, using the notation of Dieke and Crosswhite.[5] It is then evident from Eqs. (1) and (2) that

$$(P_{max}\, X)_{K=1} = -2.303 \log\left[1 - \varepsilon'(K=1) \right] . \qquad (8)$$

(2) Calculate the ratio $S_{\ell u}(K)/S_{\ell u}(K=1)$ from the expression

$$\frac{S_{\ell u}(K)}{S_{\ell u}(K=1)} = \frac{\varepsilon_u(K)\left[q_{\ell u}(K)^2\right]}{\varepsilon_u(K=1)\left[q_{\ell u}(K=1)^2\right]} \frac{\nu_{\ell u}(K)}{\nu_{\ell u}(K=1)} \left\{ \exp -\left[E_u(K) - E_u(K=1) \right]/kT \right\}$$

$$\times \left\{ \exp\left[h\nu_{\ell u}(\ell)/kT \right] - 1 \right\} \times \left\{ \exp\left[h\nu_{\ell u}(K=1)/kT \right] - 1 \right\}^{-1} . \qquad (9)$$

The first fraction appearing on the right-hand side of Eq. (9) is given by results obtained by Hill and Van Vleck[9] as written in convenient form by Earls[10] and tabulated by Dieke and Crosswhite.[5] The quantities $\nu_{\ell u}(K)$ and $E_u(K)$ have also been tabulated.[5] Relative intensities of spectral lines belonging to the P_1- and P_2- branches, (0,0)- band, $^2\Sigma \rightarrow {}^2\Pi$ transitions of OH at 3000°K are given in Table I.

(3) Determine $(P_{max}\, X)_K$ from the relation

$$(P_{max}\, X)_K = (P_{max}\, X)_{K=1} \cdot \frac{S_{\ell u}(K)}{S_{\ell u}(K=1)} \cdot \frac{\nu_{\ell u}(K=1)}{\nu_{\ell u}(K)} \qquad (10)$$

---

[9] E. Hill and J. H. Van Vleck, Phys. Rev. 32, 250 (1928).

[10] L. T. Earls, Phys. Rev. 48, 423 (1935).

and evaluate

$$\varepsilon'(K) = \left[1 - \exp -(P_{max} X)_K\right]. \qquad (11)$$

(4) Calculate

$$(I_{max})_K = \varepsilon'(K) \left[R^e (\nu_{\ell u})\right]_K. \qquad (12)$$

(5) Finally calculate $\log (I_{max})_K - \log \left\{ g_u(K) \left[\lambda_{\ell u}(K)\right]^2 \left[\nu_{\ell u}(K)\right]^3 \right\}$ and plot this quantity as a function of $E_u(K)$. From the slope of this plot determine the apparent population temperature T_u' in the usual way by applying Eq. (7).

The results of calculations carried out according to the scheme outlined above are summarized in Fig. 1 for the P_1- branch for various assumed values of $\varepsilon'(1)$, in Fig. 2 for the P_1- and P_2- branches with $\varepsilon'(1) = 0.90$ for the P_1- branch, and in Fig. 3 for the P_1- and P_2- branches with $\varepsilon'(1) = 0.50$ for the P_1- branch.

3. Discussion of Results

Analysis of the data listed in Fig. 1 leads to the conclusions enumerated below.

(1) For sufficiently small values of $\varepsilon'(1)$ the apparent and true values of the population temperatures are identical since Eq. (7) applies in good approximation. This result is, of course, well-known.

(2) As the value of $\varepsilon'(1)$ is increased, the plots constructed according to Eq. (7) show increasing curvature for the more intense rotational lines until for $\varepsilon'(1) = 0.5$ and greater the constructed curves simulate anomalous population temperatures which are of the same order of magnitude as the values reported for flames. It is easy to see how a limited number of experimental

points between K = 3 and K = 20 could be correlated by two intersecting straight lines. Apparent population temperatures T_u' obtained for lines with $10 \leq K \leq 18$ for the P_1- branch, (0,0)- band, and $^2\Sigma \rightarrow {}^2\Pi$ transitions of OH at 3000°K are listed in Table II as a function of the assumed value of $\varepsilon'(1)$.

(3) For sufficiently large values of K, all of the curves become parallel independently of the assumed values of $\varepsilon'(1)$. Thus all of the experimental data yield apparent population temperatures which are in agreement with the true value of the population temperature. Hence, by extending experimental studies to sufficiently large values of K, it is always possible to obtain unambiguous estimates of the true population temperature.

III THE EFFECT OF SELF-ABSORPTION ON APPARENT POPULATION TEMPERATURES IN ABSORPTION EXPERIMENT

At thermodynamic equilibrium the spectral emissivities and absorptivities arising from a given transition are identical. Hence it is to be expected that falsification of experimental data in absorption experiments needs to be considered whenever self-absorption is known to be of importance in emission. The following analysis is restricted to the use of peak intensities for the calculation of population temperatures.* Instrumental distortion will be neglected as in Section II.

A. Equations for the Determination of Apparent Population Temperatures

In an absorption experiment with a source which is much brighter than the emission lines and which emits the spectral radiant intensity $R_S(\nu)$, the maximum value of the fractional absorbed intensity, $\alpha' = A_{max}/R_S(\nu_{\ell u})$, is given by the expression

---

* The use of apparent total absorption measurements is discussed briefly in the Appendix II.

$$\alpha' = 1 - \exp(-P_{max} X) \tag{13}$$

whence, proceeding as for emission,

$$-\alpha' = \sum_{n=1}^{\infty} x^n/n!$$

and

$$-x = \alpha' \left[1 + \tfrac{1}{2}\alpha' + (1/3)(\alpha')^2 + (1/4)(\alpha')^3 + \cdots\right]. \tag{14}$$

For $\alpha' << 1$, Eq. (14) reduces to the expression $-x = \alpha'$ or

$$(S_{\ell u} X)\,(nc^2/2\pi k T_t \nu_{\ell u}^2)^{\frac{1}{2}} = A_{max}/R_S(\nu_{\ell u}) \tag{15}$$

where[6]

$$S_{\ell u} X \simeq (8\pi^3 N/3hc Q)\,\nu_{\ell u}\,\varepsilon_u\,q_{\ell u}^2 \left[\exp(-E_\ell/k T_\ell)\right]. \tag{16}$$

Here T_ℓ is the population temperature of the ground (initial) state in an absorption experiment. From Eqs. (15) and (16) it is readily shown[6] that for greybody emitters, with the effective temperature of the source, T_S, large compared to T_ℓ,

$$\frac{\partial \ln\left[A_{max}/\varepsilon_u\, q_{\ell u}^2\right]}{\partial E_\ell} = -\frac{1}{kT_\ell}. \tag{17}$$

It is evident that T_ℓ can, in general, be determined only if absolute values of α' are known.

B. A Method for Demonstrating the Effect of Self-Absorption on Apparent Population Temperatures of OH ($^2\Pi \rightarrow {}^2\Sigma$ Transitions)

We proceed to examine quantitatively the effect of absolute values of α' on apparent population temperatures determined according to Eq. (17).

Plots of log $\left[A_{max}/g_u\,(q_{\ell u})^2\right]$ as a function of E_ℓ can be constructed by using the following scheme.

(1) Assume a value of α', for example, for the P_1- branch, (0,0)- band, for the transition identified by the index K = 1, using the notation of Dieke and Crosswhite.[5] Next calculate $\alpha'(K)$ by using the same procedure as was used to obtain the maximum values of the spectral emissivity for the line with index K (Cf. Section II).

(2) Calculate

$$A_{max} = \alpha'(K)\, R_S\,(\nu_{\ell u}) \tag{18}$$

assuming a blackbody distribution curve for the source at the temperature T_S.

(3) Calculate log $\left\{ (A_{max})_K / g_u(K) \left[q_{\ell u}(K)\right]^2 \right\}$ and plot this quantity as a function of $E_\ell(K)$. From the slope of this plot determine the apparent population temperature T_ℓ' in the usual way by applying Eq. (17).

The results of calculations carried out according to the scheme outlined above are summarized in Figs. 4 to 7 for α' (K=1) of P_1- branch = 0.1, 0.3, 0.7, and 0.9, respectively, for two or more values of the source temperature T_S. Apparent population temperatures for the relevant assumed conditions are indicated in Figs. 4 to 7.

C. Discussion of Results

Analysis of the data presented in Figs. 4 to 7 leads to the conclusions enumerated below.

(1) Experimental data treated according to conventional procedures permit

correlation of results by linear plots even for values of α' (K=1) of the P_1- branch which are so large that T_ℓ' differs appreciably from T_ℓ. Hence absolute values obtained for T_ℓ' cannot be considered to be meaningful without convincing proof that $P_{max}X$ is sufficiently small for the spectral lines under study to justify conventional treatment of data.

(2) Apparent population temperatures T_ℓ' are always larger than T_ℓ. The difference between T_ℓ' and T_ℓ decreases somewhat as the temperature of the light source is increased, for fixed values of $P_{max}X$. However, the apparent temperatures are relatively insensitive to the numerical value of T_S, decreasing by only a few hundred degrees as T_S is raised from 3500°K to 8000°K.

(3) For sufficiently large values of α' (K=1) for the P_1- branch, discontinuities or curvatures are observed in the conventional plots which are reminiscent of the results obtained in emission experiments (Section II).

(4) Comparison with estimates of α'(K=1) based on the absolute intensity measurements performed by Oldenberg and his collaborators,[6] shows that α'(K=1) for the P_1- branch may be too large to permit the determination of rotational temperature by the use of Eq.(17) unless care is taken to utilize only spectral lines with large values of K. The particular values of K which can be used depend evidently on the [redacted] value of α'(K=1).

Adequate care in the interpretation of absorption studies, as well as of emission studies, permits the determination of both the true rotational temperature and of the concentration of the absorbing or emitting species, provided the population of molecules in the rotational energy levels obeys the Maxwell-Boltzmann distribution law. Thus data on spectral lines with large K can be used to obtain T_ℓ. Next a family of curves, for the known

values of T_{ℓ} and T_S, is constructed, for example, for different values of $\alpha'(K=1)$ for the P_1- branch (compare Figs. 4 to 7). The data obtained by using Eq. (17) for the lower values of K can then be employed to determine $\alpha'(K=1)$ whence the optical density X is determined since $S_{\ell u}$ is known.[7]

IV. THE EFFECT OF SELF-ABSORPTION ON THE USE OF ISOINTENSITY METHODS

Serious attempts to correct for the distortion of experimental data produced by self-absorption have been made by Dieke[5] and his collaborators and also by Shuler.[8] The limitations of the isointensity method and the care required in its use have been clearly stated by Dieke and Crosswhite.[5] The quantitative calculations presented here emphasize the fact that it is easy to obtain erroneous results if isointensity methods are used for the P_1- branch. It is clear that the errors will be smaller but not negligible if the isointensity methods are used for the R_2- branch, as originally proposed by Dieke and Crosswhite [5] and by Shuler.[8]

A. Outline of Calculations

Two spectral lines, which are differentiated by the indices K and K', appear to have equal peak intensities I_{max} in an emission experiment if

$$I_{max}(K) = I_{max}(K'), \tag{19}$$

where I_{max} is given by Eq. (1). For various assumed values of $\varepsilon'(K=1)$ of the P_1- branch at 3000°K, it is a simple matter to calculate the ratios $I_{max}(K)/I_{max}(K=1)$ by following the procedure described in Section II. The results of these calculations are summarized in Table III and representative values are plotted in Fig. 8.

The spectral lines, which are identified by the indices K and K', appear to have equal total intensities in emission if

$$A(K) = A(K') \tag{20}$$

where

$$A(K) = \left[R^0 \nu_{\ell u} (mc^2/2\pi kT_t)^{-\frac{1}{2}} \nu_{\ell u}(K)\right]\left[P_{max}(K)X\right] \sum_{n=0}^{\infty} \left[(n+1)^{\frac{1}{2}}(n+1)!\right]^{-1}\left[-P_{max}(K)X\right]^n . \tag{21}$$

By proceeding according to the method described in Appendix I, it is readily shown that

$$A(K)/A(K') = \left[I_{max}(K)/I_{max}(K')\right]\left[\nu_{\ell u}(K)/\nu_{\ell u}(K')\right]\left[\xi(K')/\xi(K)\right]. \tag{22}$$

Representative numerical values of $A(K)/A(K')$ are listed in Table IV and plotted in Fig. 9 for $^2\Sigma - {}^2\Pi$ transitions of OH at 3000°K for the (0,0)- band and the P_1- branch.

B. Discussion of Results

Reference to the data listed in Tables III and IV and plotted in Figs. 8 and 9 shows that the ratios $I_{max}(K)/I_{max}(K')$ and $A(K)/A(K')$ are functions of the values of $\xi'(K=1)$ for the P_1- branch, the dependence on $\xi'(K=1)$ becoming stronger as $\xi'(K=1)$ approaches unity, i.e., as the extent of self-absorption increases. This observation is emphasized by noting, for example, that the line having absolute peak intensity closest to the line with K = 3, has K = 13 for $\xi'(1) = 0.1$, K = 13 for $\xi'(1) = 0.3$, K = 14 for $\xi'(1) = 0.5$, K = 15 for $\xi'(1) = 0.7$, K = 18 for $\xi'(1) = 0.9$, K = 19 for $\xi'(1) = 0.95$, and K = 21 for $\xi'(1) = 0.99$. Comparison of the data given in Tables III and IV and plotted in Figs. 8 and 9, respectively, also shows that the effect of self-absorption in falsifying the data obtained by use of the isointensity method is more pronounced for peak emitted intensities than for total intensities.

The effect of self-absorption on population temperatures determined from the isointensity method can be demonstrated graphically by using the procedure developed by Shuler[8] whose method is equivalent to the assumption that total intensity ratios $A(K)/A(K')$ can be replaced by the product of transition probability ratios $g_u(K)\left[q_{\ell u}(K)\right]^2 / g_u(K')\left[q_{\ell u}(K')\right]^2$ and appropriate exponential factors for spectral lines which are close together. Plots of $E(K) - E(K')$ vs. $\log\left\{ g_u(K)\left[q_{\ell u}(K)\right]^2 / g_u(K')\left[q_{\ell u}(K')\right]^2 \right\}$ are shown in Fig. 10 as a function of $\xi'(1)$ for pairs of spectral lines for which $I_{max}(K)/I_{max}(K')$ is nearly equal to unity. Similarly, plots of $E(K) - E(K')$ vs. $\log\left\{ g_u(K)\left[q_{\ell u}(K)\right]^2 / g_u(K')\left[q_{\ell u}(K')\right]^2 \right\}$ are shown in Fig. 11 as a function of $\xi'(1)$ for pairs of spectral lines for which $A(K)/A(K')$ is nearly equal to unity.

Reference to Figs. 10 and 11 shows that the plots deviate progressively more from straight lines as $\xi'(1)$ is increased. Apparent population temperatures T_u' are noted on the curves given in Figs. 10 and 11. The results are seen to be an immediate consequence of the dependence of the K-values for lines with equal peak or total intensities on $\xi'(1)$. Hence the conclusion is reached that the effects of self-absorption in distorting experimental data do not necessarily cancel in first order for the isointensity methods. A simple physical explanation for failure of the isointensity methods at large values of the spectral emissivity is obtained by noting that the quantities $R^o(\nu_{\ell u})$ influence the observable intensities and that $R^o(\nu_{\ell u})$, which is a function of temperature, is not the same for any distinguishable pair of spectral lines. Furthermore, equally intense spectral lines, for which $S_{\ell u}(K) = S_{\ell u}(K')$, have slightly different widths since

the Doppler width is proportional to the frequency of the line center. Thus the obvious conclusion is reached that the effects of self-absorption will cancel exactly only for equally intense spectral lines with line centers occurring at identical frequencies.

V. ERRORS IN CONVENTIONAL PROCEDURES FOR ISOTHERMAL SYSTEMS IN THE ABSENCE OF SELF-ABSORPTION

Whereas the effect of self-absorption in producing distortion of emission data has been amply discussed, relatively little analytical work has been done on the meaning of discontinuous curves for a mixture of isothermal systems in the absence of self-absorption. Although the methods of calculation which we employ are well-known and the conclusions to which they lead are almost obvious, it is somewhat surprising to note that errors in interpretation can be made even for the often postulated non-equilibrium distribution of OH. Aside from emphasizing the need for care in dealing with anything other than a linear plot, the present analysis also serves to give examples of linear isointensity plots of the Shuler-type[8] for the P_1- branch with meaningless temperatures for a non-equilibrium distribution of OH. Whether or not the R_2- branch is quite as bad can be said with assurance only after quantitative calculations have been carried out; however, we expect the errors to be less pronounced. In this connection reference should be made also to the discussion of the isointensity method given by Dieke and Crosswhite,[5] who indicate very clearly under what conditions the method is usable.

A. Outline of Theory

For a non-equilibrium mixture of gases containing OH at 3000°K and at 6000°K, the total observable intensity A(K) emitted from the spectral line identified by the index K with line center at $\nu_{\ell_u}(K)$ is given by the expression

$$A(K)/(c/4) = \left\{ \int^{\circ} \left[\nu_{\ell u}(K) \right] \; S_{\ell u}(K) X \right\}_{T=3000^{\circ}K} + \left\{ \int^{\circ} \left[\nu_{\ell u}(K) \right] \; S_{\ell u}(K) X \right\}_{T=6000^{\circ}K} \quad (23)$$

where the effects of self-absorption have been assumed to be negligible. The total intensity of the line with index K divided by the total intensity of the line with index K = 1 is

$$G = A(K)/A(1) = \left[B(T = 6000) + B(T = 3000) C \right] / (1 + C) \quad (24)$$

where

$$B(T) = \left\{ \int^{\circ} \left[\nu_{\ell u}(K) \right] \; S_{\ell u}(K) / \int^{\circ} \left[\nu_{\ell u}(1) \right] \; S_{\ell u}(1) \right\}_{T}$$

$$= \left[\nu_{\ell u}(K) / \nu_{\ell u}(1) \right]^{4} \left[(g_u q_{\ell u}^{2})_K / (g_u q_{\ell u}^{2})_1 \right] \times \exp \left\{ - \left[E_u(K) - E_u(1) \right] / kT \right\} \quad (25)$$

and

$$C = \left\{ \int^{\circ} \left[\nu_{\ell u}(1) \right] \; S_{\ell u}(1) X \right\}_{T=3000} \Big/ \left\{ \int^{\circ} \left[\nu_{\ell u}(1) \right] \; S_{\ell u}(1) X \right\}_{T=6000}$$

$$= \left(X_{3000} / X_{6000} \right) \left[\exp - \left\{ E_u(1)/k \left[(1/3000) - (1/6000) \right] \right\} \right] . \quad (26)$$

The non-equilibrium character of the OH distribution is expressed by the non-zero and non-infinite ratio

$$r = X_{3000} / X_{6000} . \quad (27)$$

For r = 0 the present discussion reduces to the analysis of an isothermal system at 6000°K whereas for 1/r = 0, the radiation becomes that characteristic of an isothermal system at 3000°K. It is apparent that r must be considerably

greater than unity before the OH with rotational temperature at 3000°K will influence the observed radiation from the non-equilibrium mixture.

The apparent temperatures which would be obtained from observations of the mixture if conventional treatment of emission data were employed, is obtained by plotting $\log \left\{ G/\left[\nu_{\ell u}(K)/\nu_{\ell u}(1)\right]^4 \left[(\varepsilon_u q_{\ell u}{}^2)_K / (\varepsilon_u q_{\ell u}{}^2)_1\right]\right\}$ as a function of $E_u(K)$. Similarly, isointensity plots may be constructed according to the method of Shuler[8] by noting that for equally intense lines with indeces K and K', respectively, $G(K) = G(K')$.

B. Discussion of Results

Interpretation of measured intensities according to conventional procedures for analysis of emission data is illustrated in Figs. 12 to 18. In accord with expectations, we find for $r \leq 10^2$ that the observable intensity ratios are practically those characteristic of an isothermal system at 6000°K. On the other hand, for $r \geq 10^6$, the non-equilibrium mixture radiates almost like an isothermal system at 3000°K. For intermediate values of r, intensities are obtained in the usual logarithmic plots (Cf. Figs. 12 to 18) which can be represented, in adequate approximation, by two intersecting straight lines. For low values of K temperatures greater than 3000°K are obtained whereas for high values of K temperatures lower than 6000°K are obtained. Of particular interest is the fact that data calculated according to Shuler's isointensity method (Cf. Figs. 19 to 21) can frequently be correlated by linear plots even under conditions in which conventional procedures clearly show discontinuities.* Of course, the slopes derived from Shuler's isointensity plots are meaningless in these cases. The data

---

* There are several obvious reasons for this result. Thus, without applying a suitable frequency correction or using interpolation between listed values of K, there is considerable intrinsic scatter in the isointensity plots. Furthermore, the number of points which can be used to draw the final plot is reduced to one half. Hence it is quite possible to obtain isointensity plots which do not show the finer details of conventional plots.

shown in Figs. 12 to 18 are notable also in that they show a less marked difference between the apparent temperatures for low and high values of K than is usually obtained experimentally. This observation, together with the fact that the apparent population temperatures are always too high, certainly indicates that as long as non-linear plots are obtained a simple interpretation of observable data is inadmissable even for a mixture of isothermal systems in the absence of self-absorption. Thus, two intersecting straight lines with apparent temperatures T_1 and T_2 can be obtained only by non-equilibrium mixtures at temperatures other than T_1 and T_2.

VI. APPARENT TEMPERATURES FOR TWO ADJACENT ISOTHERMAL REGIONS

The observable radiation from real flames is always produced as the result of a non-isothermal field of view. Without a detailed prescription of temperature and concentration gradients along the line of sight it is not possible to incorporate quantitative corrections in the interpretation of experimental data. However, it is apparent that the falsification of data in conventional plots will be similar to the falsification produced by self-absorption as long as a hot region is viewed through a cooler gas layer. We shall demonstrate this conclusion by representative calculations on the observable emitted radiation for spectral lines with Doppler contour when an isothermal region at 3000°K is viewed through an isothermal region at 1500°K. The concentrations of emitter in the two regions will be treated as variable parameters. Although we present theoretical results only for the P_1- branch, it is clear from a study of the factors responsible for distortions produced by observations through cooler gas layers that, for example, the R_2 - branch will be modified in roughly the same manner as the P_1- branch. Hence, although the use of isointensity methods is advantageous

in minimizing the effects of self-absorption for the R_2- branch, the use of the R_2- branch becomes less significant if distortion by temperature gradients is also of importance. It is gratifying to note, however, that the distortions resulting from temperature gradients are reduced if the extent of self-absorption is diminished.

A. Outline of Theory for Peak Intensities

Consider an isothermal region at temperature T with properties X, P_ν, P_{max}, $R(\nu_{\ell u})$, and $\varepsilon = 1 - \exp(-P_{max}X)$ which is observed through an isothermal region at temperature T' with properties X', P_ν', P_{max}', $R'(\nu_{\ell u})$, and $\varepsilon' = 1 - \exp(-P_{max}' X')$. The maximum observable intensity for the spectral line whose center lies at the frequency $\nu_{\ell u}$ is

$$I_{max} = R(\nu_{\ell u}) \left\{ \varepsilon + \exp(-h\nu_{\ell u}/k) \left[(1/T') - (1/T)\right] \right\}^{[\varepsilon'/(1-\varepsilon')]K} (1-\varepsilon'). \quad (28)$$

A conventional plot for the study of emission experiments can be constructed according to the scheme outlined below.

(1) For $T = 3000^\circ K$ and $T' = 1500^\circ K$ and fixed values of $\varepsilon(K=1)$ and $\varepsilon'(K=1)$ for the P_1- branch calculate $(P_{max}X)_{K=1}$ and $(P_{max}'X')_{K=1}$.

(2) Calculate the ratios $S_{\ell u}(K,T)/S_{\ell u}(K=1,T)$ and $S_{\ell u}'(K,T')/S_{\ell u}'(K=1,T')$.

(3) Calculate $(P_{max}X)_K$ and $(P_{max}'X')_K$ and hence $\varepsilon(K)$ and $\varepsilon'(K)$.

(4) Determine I_{max} from Eq. (28) and plot $\log\left[I_{max}/(\varepsilon_u q_{\ell u}^2)(\nu_{\ell u})^3\right]$ as a function of $E_u(K)$.

B. Discussion of Results for Peak Intensities

The results of numerical calculations are summarized in Figs. 22 to 24 for $\varepsilon(K=1) = 0.3$, 0.5, 0.7, and 0.9, respectively, for varying values of $\varepsilon'(K=1)$ with $\varepsilon'(K=1) \leq \varepsilon(K=1)$. Reference to Figs. 22 to 24 clearly

shows that observations through a cool isothermal region accentuate the distortion observed for self-absorption alone. For example, for $\varepsilon\,(K=1) = \varepsilon'\,(K=1) = 0.3$ a definite curvature is observed (Cf. Fig. 22) whereas for $\varepsilon\,(K=1) = 0.3$ and $\varepsilon'\,(K=1) = 0$ a linear plot with a nearly "normal" temperature obtains (Cf. Fig. 1). For strong self-absorption both in the hotter and cooler gas layers, extensive self-reversal may occur[11] leading to no real values for the "temperature" (Cf. Figs. 23 to 25).

It should perhaps be emphasized that the data shown in Figs. 22 to 25 are only of qualitative significance in so far as application to real flames is concerned. Furthermore, the results are, of course, modified if appropriate plots for total intensities are used instead of plots for peak intensities. In general one would expect the extent of distortion to be somewhat diminished for total intensity measurements. Detailed calculations will not be presented here since the precise evaluation of the integrals involved is somewhat laborious and since the results would add little to the qualitative conclusions stated above.

VII. APPLICATION TO FLAMES

It is evident that none of the quantitative results presented for idealized systems in Sections II to VI apply to real flames. Nevertheless it is perhaps justifiable to perform some extrapolation to real systems.

To begin with, it is clear that observed "anomalies" <u>can be</u> explained by distortion of experimental data through self-absorption and/or temperature gradients. In order to make observable anomalies appear real it is therefore necessary to perform experiments proving that distortion of data does not play a significant role. The proof should be direct and not inferential.

---

[11] R. D. Cowan and G. H. Dieke, Revs. Mod. Phys. <u>20</u>, 418 (1948).

In order to emphasize the fact that inferential proof may be no proof at all we consider, for example, an isothermal system at 3000°K with $\mathcal{E}'(1) = 0.70$ for the P_1- branch. Conventional interpretation of emission experiments (Cf. Fig. 1) will then show experimental data which can be correlated by intersecting straight lines leading to a value of $T_u' \simeq 5000°K$ for the $^2\Sigma$ - state for $10 \leq K \leq 20$ (Cf. Table II). Next absorption experiments are performed with a light source at 8000°K and, considering the inevitable scatter of experimental data, the observed results are well correlated by a single straight line with $T_\ell' \simeq 3650°K$ (Cf. Fig. 6). On the basis of these experimental results, one could argue with vigor for a nearly "normal" distribution of OH in the ground ($^2\Pi$) state and for abnormal excitation of OH in the excited ($^2\Sigma$) state. For the case under discussion, in spite of the seemingly convincing inferential evidence, the conclusion would obviously be erroneous.

We have presented previously[12] a critical review of available experimental evidence for anomalous population temperatures in flames in which we emphasized the lack of unequivocal evidence either for or against the reality of the anomalies, noting, however, the wealth of inferential evidence, in favor of a non-equilibrium distribution of OH, presented by Gaydon and Wolfhard.[1] We did not intend to replace a temperature anomaly by a concentration anomaly. Rather we were interested only in showing that as yet the experimental evidence is not sufficiently clear to warrant quantitative interpretation. We have proposed a two-path method which eliminates all errors arising from self-absorption in isothermal systems for spectral lines with Doppler contour.[13] However, we do not consider the method to be exactly valid for the study of regions of active combustion. The only conclusion which we feel

---

12 S. S. Penner, J. Chem. Phys. 20, August (1952).

13 S. S. Penner, J. Chem. Phys. 20, August (1952).

justified in stating at the present time is that the spectroscopic study of regions of active combustion is useful for species identification and may, in time, lead to a valid quantitative picture, for example, of OH rotational temperatures and OH concentrations. The final analysis may prove or disprove the reality of anomalies. However, we shall find such proof convincing only if every precaution has been taken to eliminate instrumental errors and all necessary corrections for distortions have been made by a realistic study of temperature gradients and of the extent of self-absorption. In this connection we wish to emphasize again the fact that the use of the isointensity method for the R_2- branch, with proper consideration for all of the precautions mentioned by Dieke,[5] will minimize self-absorption errors. However, the use of the R_2- branch is not sufficient to eliminate the coupled effects of self-absorption and temperature gradients (compare Section VI).

The question of the reality or fiction of anomalous rotational, vibrational, and electronic temperatures for OH in flames is of practical importance in connection with the development of rigorous theories of one-dimensional laminar flame propagation.[14] A review of observed anomalies shows uniformly high population temperatures not only for OH but also for other chemical species. On the other hand, theoretical studies by Golden and Peiser show a low rotational temperature for newly formed HBr.[15] If non-equilibrium distributions persist in flames, the attempts at a rigorous calculation of burning velocities for one-dimensional flame propagation are enormously complicated because of our completely inadequate knowledge of detailed reaction mechanisms, particularly between molecules and radicals in excited

---

[14] J. O. Hirschfelder and C. F. Curtiss, J. Chem. Phys. 17, 1076 (1949).

[15] S. Golden and A. M. Peiser, J. Chem. Phys. 17, 630 (1949).

states. The hypothesis that spectroscopic investigations yield information about side reactions and can therefore be ignored in a realistic formulation of the detailed reaction steps in flames is not altogether satisfying since energy must be conserved and we have as yet no detailed knowledge concerning energy-deficient chemical species in the reaction zones of flames. For this reason, continued spectroscopic studies of flames are of interest not only in ascertaining details concerning the particular reaction steps which can be studied conveniently, but they also have a bearing on such parameters as the linear burning velocity, etc.

In conclusion, the author takes pleasure in expressing his appreciation to Drs. O. R. Wulf and H. S. Tsien for helpful comments. The numerical work was performed by E. K. Björnerud and R. W. Kavanagh.

APPENDIX I. BASIC RELATIONS IN TERMS OF TOTAL EMITTED INTENSITIES

The expressions given in Section II require slight modifications when total intensity ratios rather than peak intensity ratios are available. If the apparent integrated intensity of the spectral line with center at the frequency $\nu_{\ell u}$ is denoted by the symbol $A(\nu_{\ell u})$, then, as is well-known,*

$$A(\nu_{\ell u}) \simeq R^{o}(\nu_{\ell u})(mc^2/2\pi kT_t \nu_{\ell u}^2)^{-\frac{1}{2}} (P_{max}X)\left\{\sum_{n=0}^{\infty} \left[(n+1)^{\frac{1}{2}}(n+1)!\right]^{-1} (-P_{max}X)^n\right\}. \quad (A-1)$$

From Eqs. (1) and (A-1) it follows that

$$I_{max} = \left[A(\nu_{\ell u})/\nu_{\ell u}\right](mc^2/2\pi kT_t)^{\frac{1}{2}} \gamma \quad (A-2)$$

where

$$\gamma = \left\{(P_{max}X)\sum_{n=0}^{\infty}\left[(n+1)^{\frac{1}{2}}(n+1)!\right]^{-1}(-P_{max}X)^n\right\}^{-1}\left[1 - \exp(-P_{max}X)\right]. \quad (A-3)$$

Since $\gamma = 1$ for $P_{max}X \ll 1$, it is apparent from Eqs. (7) and (A-2) that

$$\frac{\partial \ell n\left[A(\nu_{\ell u})/\nu_{\ell u}^4 g_u (q_{\ell u})^2\right]}{\partial E_u} = -\frac{1}{kT_u} \quad \text{for } \xi' \ll 1 \text{ for all lines.} \quad (A-4)$$

Equation (A-4) is the expression which is usually employed for the interpretation of experimental data. The value of γ is plotted as a function of $P_{max}X$ in Fig.(A-1).

When conventional plots for the determination of population temperatures are constructed according to Eq. (A-4) for arbitrary values of ξ' (1), results substantially equivalent to those shown in Fig. 1 are obtained. In this case the quantity $A(\nu_{\ell u})$ can be calculated from Eq. (A-2) after obtaining I_{max} by use of the procedure described in Section IIB. Construction of

---

* R. Ladenburg, Zeits. f. Physik 65, 200 (1930).

curves analogous to those shown for the P_1- and P_2- branches in Figs. 2 and 3 leads to the conclusion that the separation between lines belonging to the P_1- and P_2- branches is slightly decreased.

APPENDIX II. POPULATION TEMPERATURES BASED ON APPARENT TOTAL ABSORPTION MEASUREMENTS FOR SPECTRAL LINES WITH DOPPLER CONTOUR

It is readily shown that the apparent total absorption A_T is related to the peak absorption A_{max} through the expression

$$A_{max} = A_T \cdot \mathfrak{F} \cdot (\nu_{\ell u})^{-1} (mc^2/2\pi kT_t)^{\frac{1}{2}} \qquad (A-5)$$

where $\mathfrak{F}$ is given by Eq. (A-3). By the use of Eqs. (A-3) and (A-5) it is a simple matter to convert the data given in Figs. 4 to 7 to the corresponding plots involving A_T. The values of $\mathfrak{F}$ as a function of P_{max} X have been given in Fig. (A-1). Conclusions derived from conventional plots in terms of A_T for estimating population temperatures do not differ significantly from the material given in Section III, for the range of spectral emissivities considered in the present analysis.

LIST OF FIGURES

LIST OF FIGURES

Fig. 6 Conventional plots for the determination of apparent population temperatures T_ℓ' of the ground electronic state from absorption experiments for different temperatures of the light source T_S [$^2\Pi \rightarrow {}^2\Sigma$ transitions of OH, (0,0)- band, P_1- branch, $T = 3000^\circ K$, $\alpha'(1) = 0.70$].

Fig. 7 Conventional plots for the determination of apparent population temperatures T_ℓ' of the ground electronic state from absorption experiments for different temperatures of the light source T_S [$^2\Pi \rightarrow {}^2\Sigma$ transitions of OH, (0,0)- band, P_1- branch, $T = 3000^\circ K$, $\alpha'(1) = 0.90$].

Fig. 8 The ratio $I_{max}(K)/I_{max}(1)$ as a function of K for the P_1- branch, (0,0)- band, $^2\Sigma \rightarrow {}^2\Pi$ transitions of OH at $3000^\circ K$ for different values of $\varepsilon'(1)$.

Fig. 9 The ratio A(K)/A(1) as a function of K for the P_1- branch, (0,0)- band, $^2\Sigma \rightarrow {}^2\Pi$ transitions of OH at $3000^\circ K$ for different values of $\varepsilon'(1)$.

Fig. 10 Plot of $[E_u(K) - E_u(K')]$ vs. $\log\left\{ g_u(K)\left[q_{\ell u}(K)\right]^2 / g_u(K')\left[q_{\ell u}(K')\right]^2 \right\}$ for lines with equal peak intensities at $3000^\circ K$ as a function of $\varepsilon'(1)$ for the P_1- branch, (0,0)- band, $^2\Sigma \rightarrow {}^2\Pi$ transitions of OH.

Fig. 11 Plot of $[E_u(K) - E_u(K')]$ vs. $\log\left\{ g_u(K)\left[q_{\ell u}(K)\right]^2 / g_u(K')\left[q_{\ell u}(K')\right]^2 \right\}$ for lines with equal total intensities at $3000^\circ K$ as a function of $\varepsilon'(1)$ for the P_1- branch, (0,0)- band, $^2\Sigma \rightarrow {}^2\Pi$ transitions of OH.

Fig. 12 Conventional plots and apparent temperatures for various bimodal distributions of OH.

Fig. 13 Conventional plot and apparent temperatures for $r = 5 \times 10^2$.

Fig. 14 Conventional plot and apparent temperatures for $r = 10^3$.

Fig. 15 Conventional plot and apparent temperatures for $r = 2 \times 10^3$.

Fig. 16 Conventional plot and apparent temperatures for $r = 4 \times 10^3$.

Fig. 17 Conventional plot and apparent temperatures for $r = 6 \times 10^3$.

Fig. 18 Conventional plot and apparent temperatures for $r = 8 \times 10^3$.

Fig. 19 Isointensity plots and apparent temperatures for $r = 5 \times 10^2$, 1×10^3, and 2×10^3.

Fig. 20 Isointensity plots and apparent temperatures for $r = 4 \times 10^3$, 6×10^3, and 8×10^3.

Fig. 21 Isointensity plots and apparent temperatures for $r = 10^2$, 10^4, and 10^6.

Fig. 22 Conventional plots for the interpretation of emission experiments with two adjacent isothermal regions at 1500 and 3000°K, respectively, for $\xi(X = 1) = 0.3$ for the P_1- branch.

Fig. 23 Conventional plots for the interpretation of emission experiments with adjacent isothermal regions at 1500 and 3000°K, respectively, for $\xi(X = 1) = 0.5$ for the P_1 - branch.

Fig. 24 Conventional plots for the interpretation of emission experiments with two adjacent isothermal regions at 1500 and 3000°K, respectively, for: $\varepsilon\,(K = 1) = 0.7$ for the P_1- branch.

Fig. 25 Conventional plots for the interpretation of emission experiments with two adjacent isothermal regions at 1500 and 3000°K, respectively, for $\varepsilon\,(K = 1) = 0.9$ for the P_1- branch.

Fig. (A-1) The quantity $\bar{\varepsilon}$ as a function of P_{max} X.

Figs. (1) to (3) correspond to Figs. (1) to (3) of Part I in T.R. #5.

Figs. (4) to (7) correspond to Figs (1) to (4) of Part II in T.R. #5

Figs. (8) to (11) correspond to Figs. (1) to (4) of Part III in T.R. #5

Fig. (A-1) corresponds to Fig. (A-1) of Part I in T.R. #5.

Tables I and II correspond to Tables I and II of Part I in T.R. #5.

Tables III and IV correspond to Tables ~~III~~ I and ~~IV~~ II of Part III in T.R. #5.

Figure 12

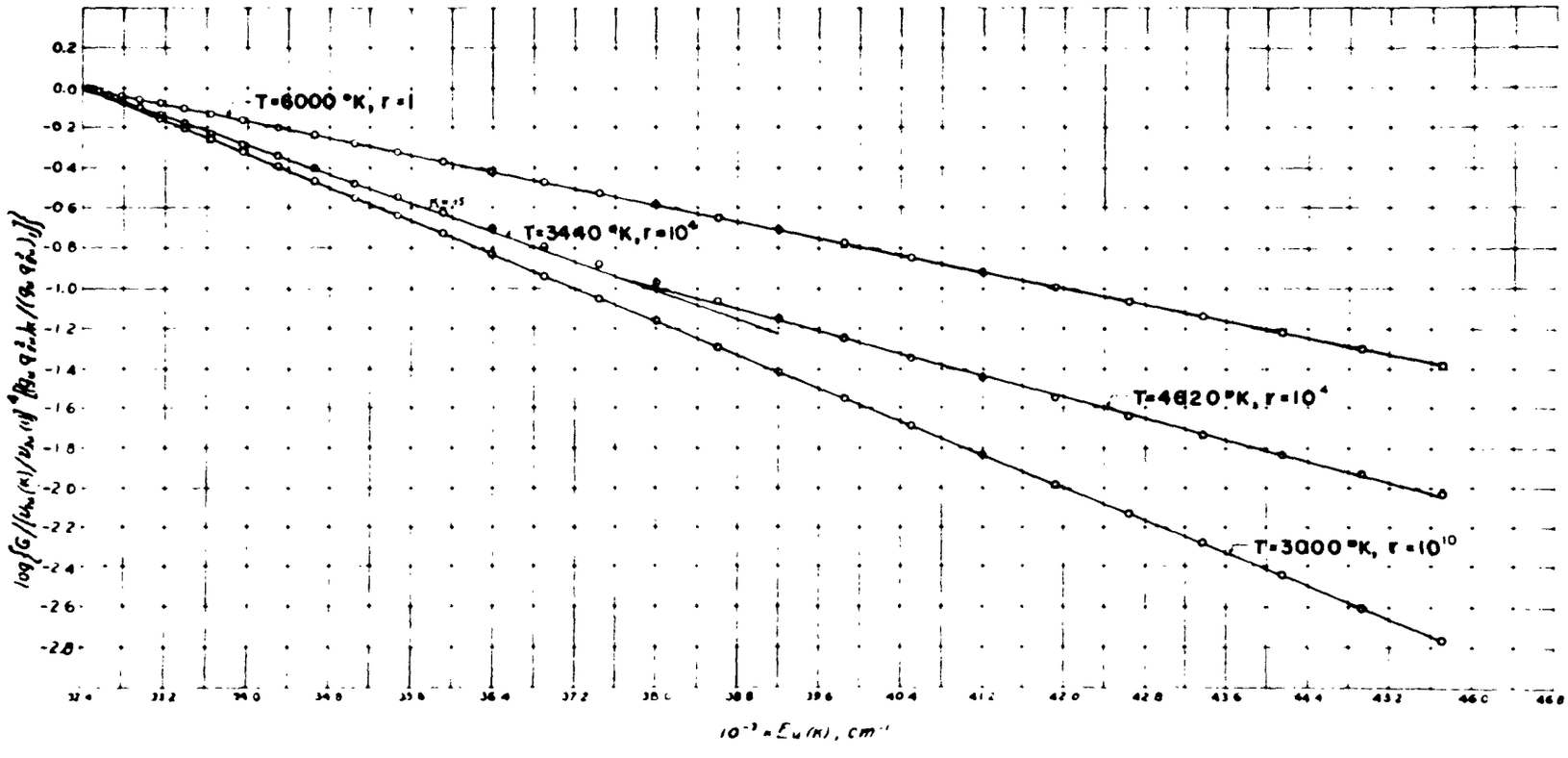
T=6000 °K, r=1
T=3440 °K, r=10^5
T=4820 °K, r=10^4
T=3000 °K, r=10^10
0.2
0.0
-0.2
-0.4
-0.6
-0.8
-1.0
-1.2
-1.4
-1.6
-1.8
-2.0
-2.2
-2.4
-2.6
-2.8
32.4
33.2
34.0
34.8
35.6
36.4
37.2
38.0
38.8
39.6
40.4
41.2
42.0
42.8
43.6
44.4
45.2
46.0
46.8
10^-3 = E_u(K), cm^-1

Figure 13

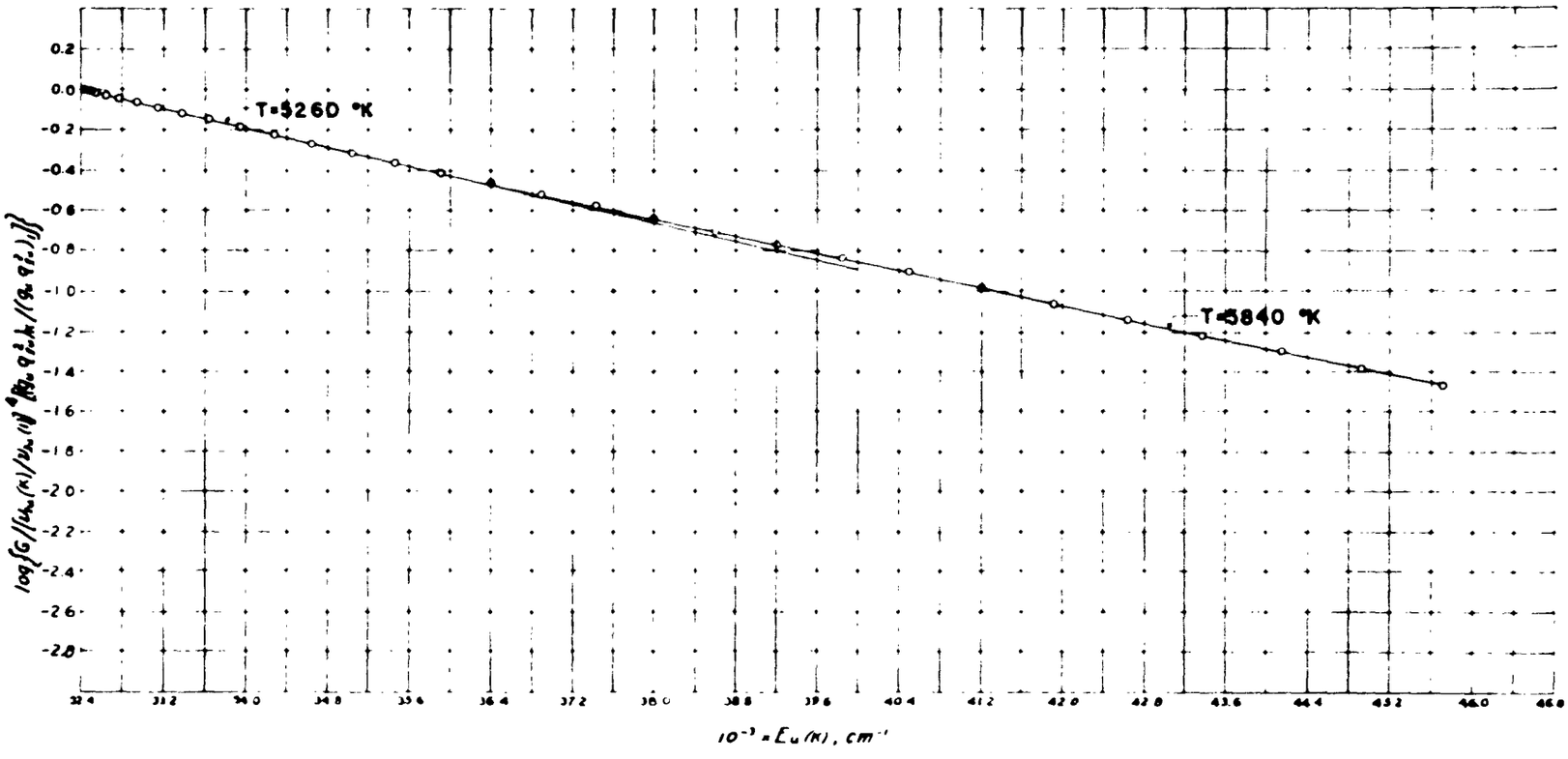
T=526D °K
T=5840 °K
0.2
0.0
-0.2
-0.4
-0.6
-0.8
-1.0
-1.2
-1.4
-1.6
-1.8
-2.0
-2.2
-2.4
-2.6
-2.8
32.4
33.2
34.0
34.8
35.6
36.4
37.2
38.0
38.8
39.6
40.4
41.2
42.0
42.8
43.6
44.4
45.2
46.0
46.8
$10^{-3} = E_u(K)$, cm^{-1}

Figure 14

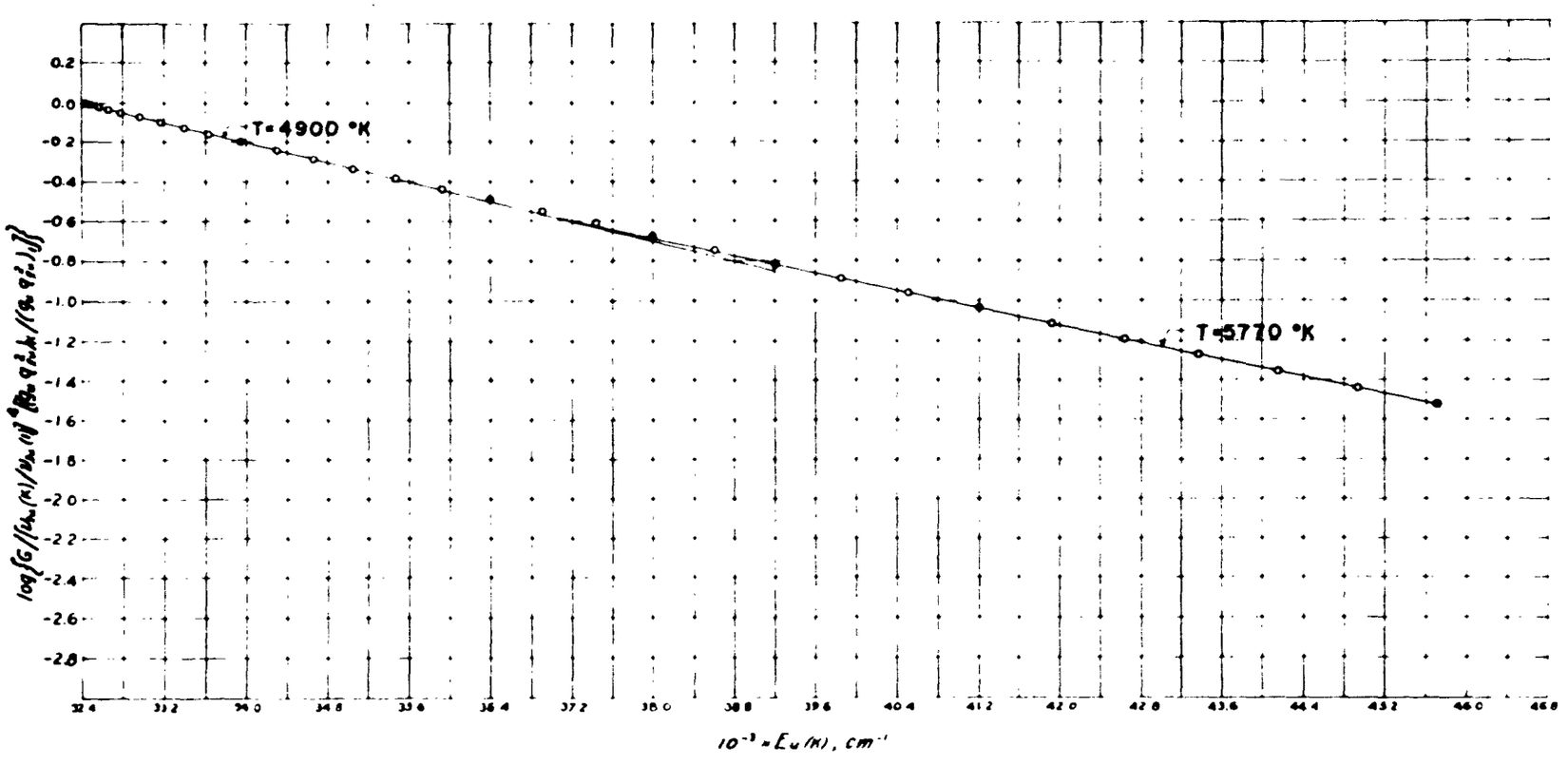
T=4900 °K
T=5770 °K
0.2
0.0
-0.2
-0.4
-0.6
-0.8
-1.0
-1.2
-1.4
-1.6
-1.8
-2.0
-2.2
-2.4
-2.6
-2.8
32.4
33.2
34.0
34.8
35.6
36.4
37.2
38.0
38.8
39.6
40.4
41.2
42.0
42.8
43.6
44.4
45.2
46.0
46.8
$10^{-3} \times E_u(K)$, cm^{-1}

Figure 15

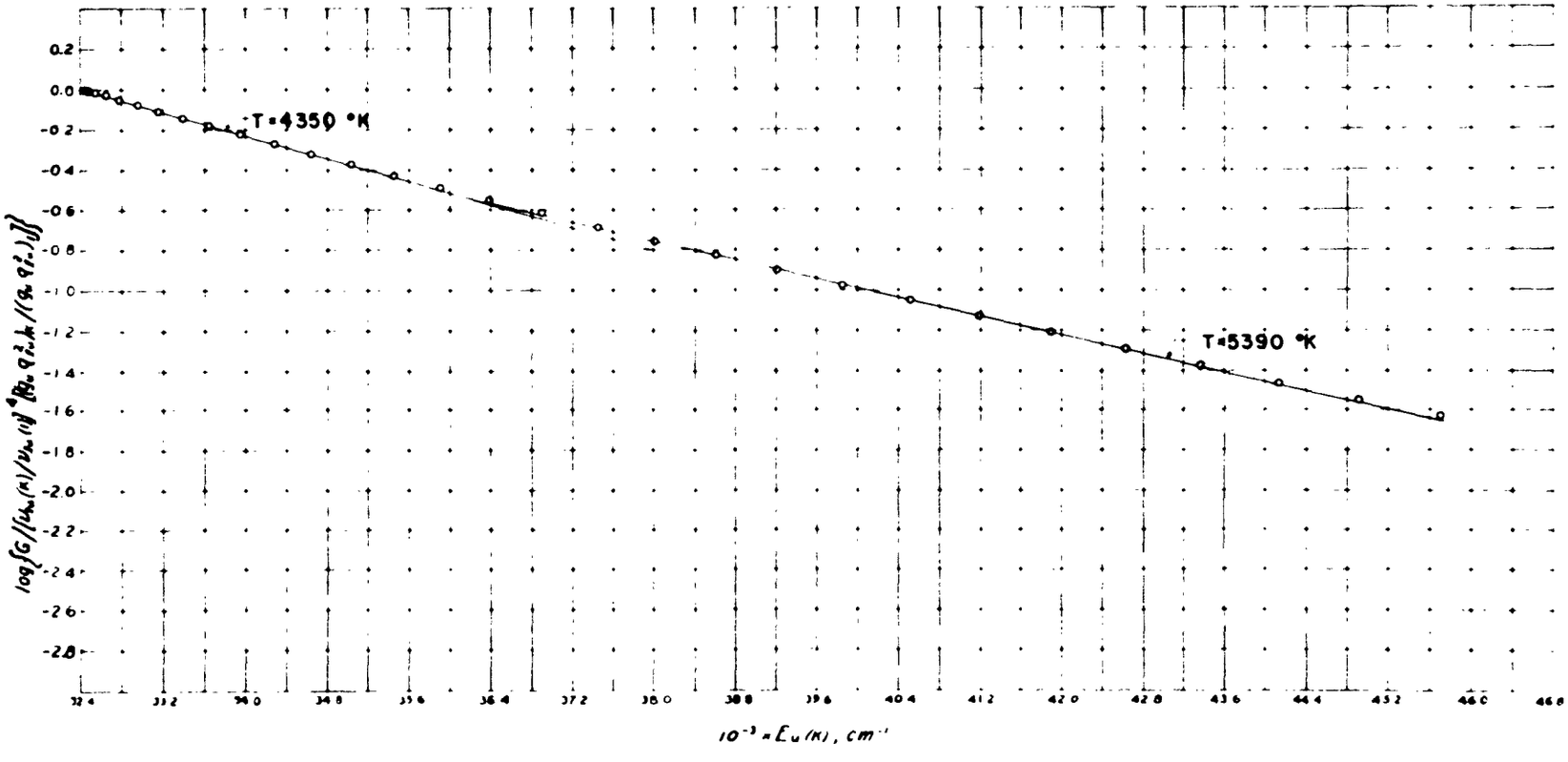
T=4350 °K
T=5390 °K
0.2
0.0
-0.2
-0.4
-0.6
-0.8
-1.0
-1.2
-1.4
-1.6
-1.8
-2.0
-2.2
-2.4
-2.6
-2.8
32.4
33.2
34.0
34.8
35.6
36.4
37.2
38.0
38.8
39.6
40.4
41.2
42.0
42.8
43.6
44.4
45.2
46.0
46.8
$10^{-3} \times E_u(K)$, cm^{-1}

Figure 16

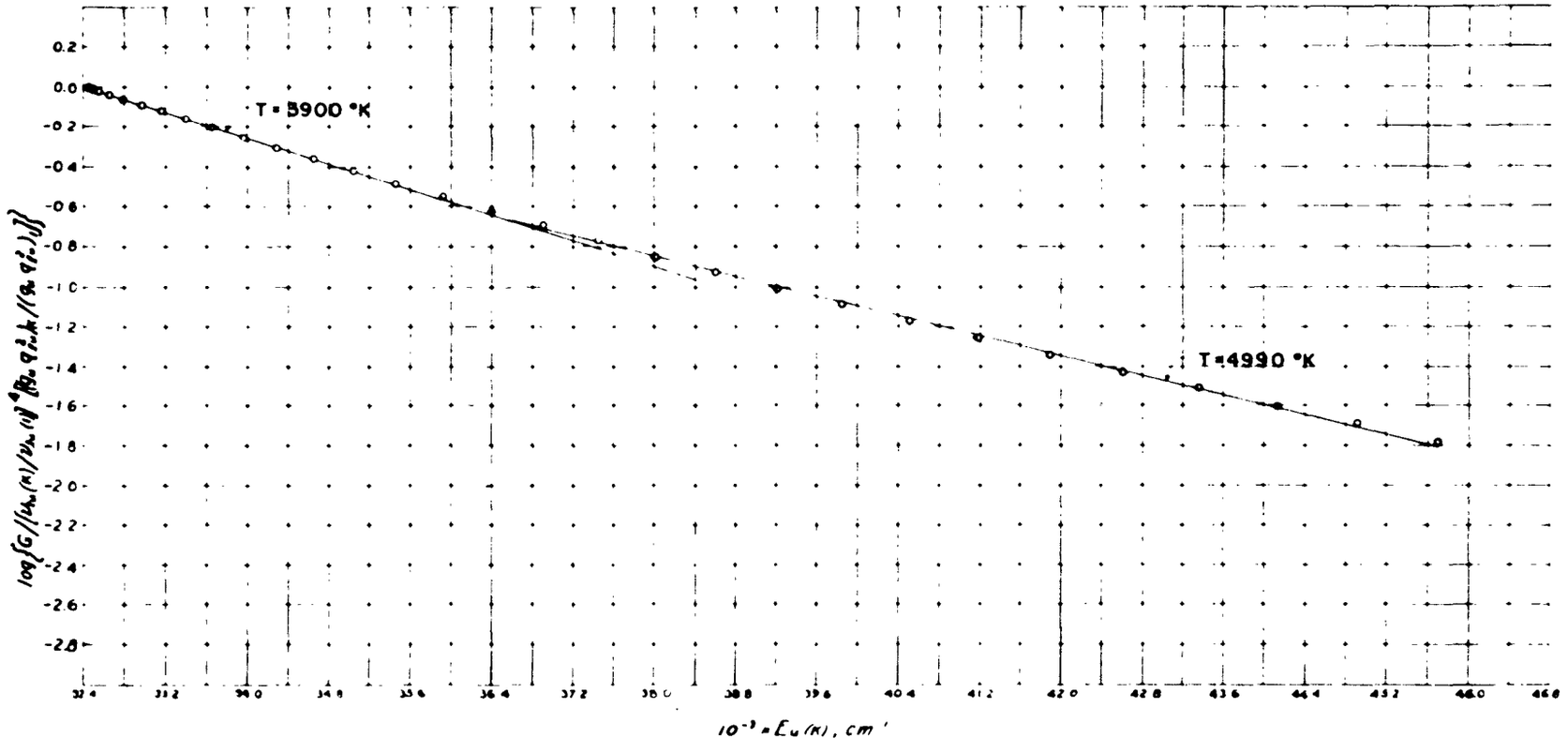
T = 5900 °K
T = 4990 °K
0.2
0.0
-0.2
-0.4
-0.6
-0.8
-1.0
-1.2
-1.4
-1.6
-1.8
-2.0
-2.2
-2.4
-2.6
-2.8
32.4
33.2
34.0
34.8
35.6
36.4
37.2
38.0
38.8
39.6
40.4
41.2
42.0
42.8
43.6
44.4
45.2
46.0
46.8
$10^{-3} \cdot E_u(K)$, cm^{-1}

Figure 17

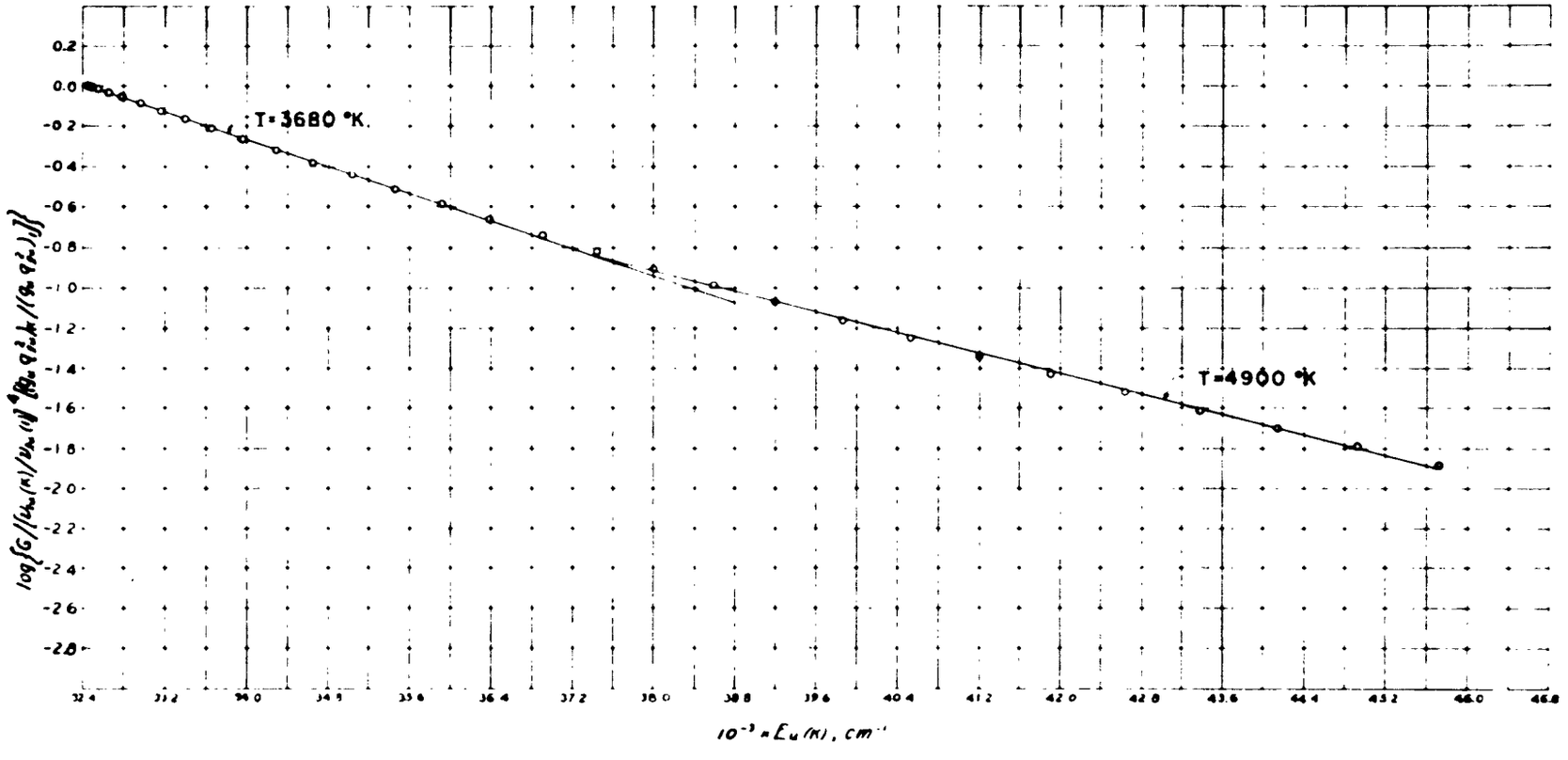
T=3680 °K.
T=4900 °K
0.2
0.0
-0.2
-0.4
-0.6
-0.8
-1.0
-1.2
-1.4
-1.6
-1.8
-2.0
-2.2
-2.4
-2.6
-2.8
32.4
33.2
34.0
34.8
35.6
36.4
37.2
38.0
38.8
39.6
40.4
41.2
42.0
42.8
43.6
44.4
45.2
46.0
46.8
$10^{-3} \times E_u(K)$, cm^{-1}

Figure 18

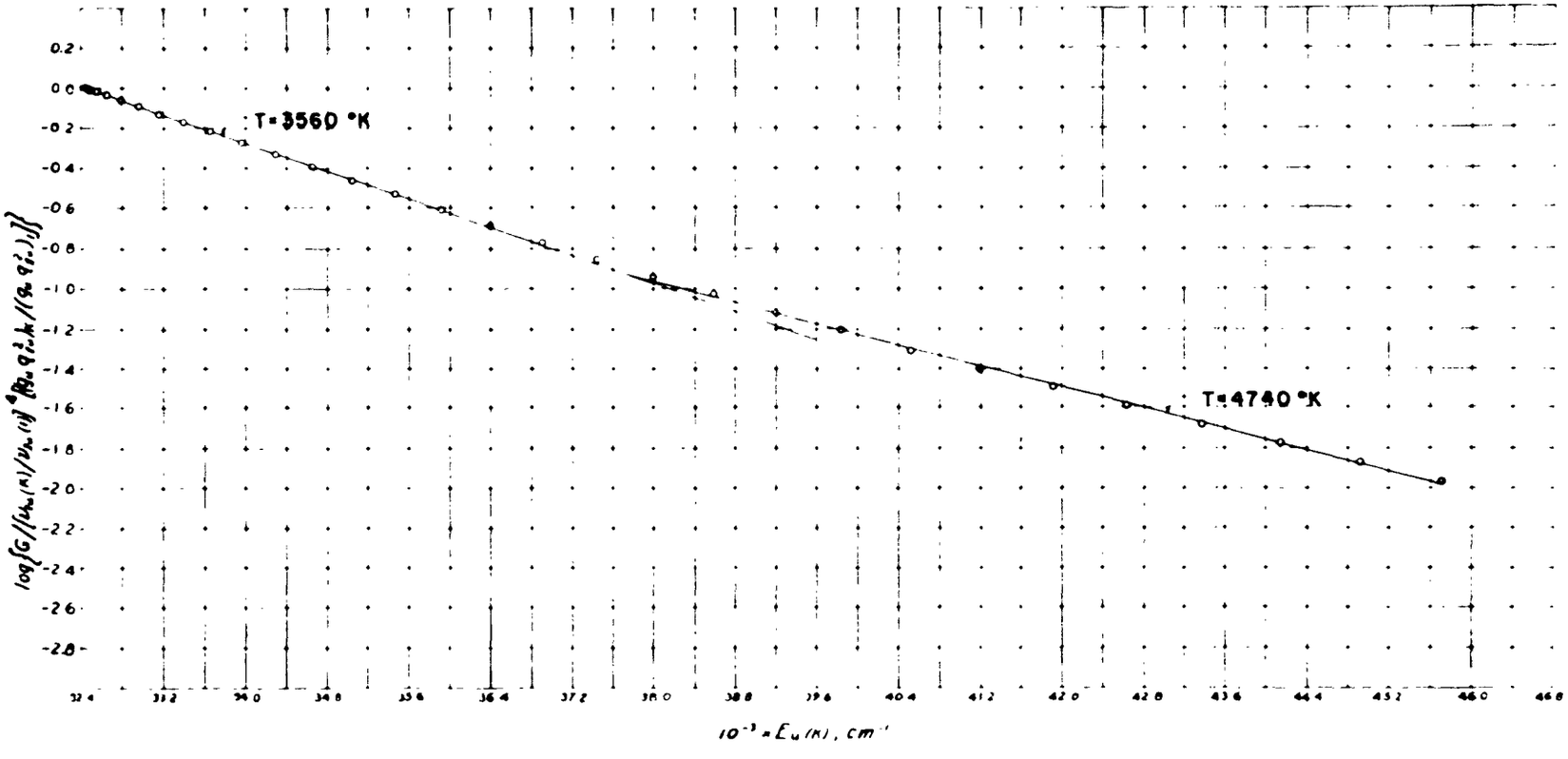
T=3560 °K
T=4740 °K
0.2
0.0
-0.2
-0.4
-0.6
-0.8
-1.0
-1.2
-1.4
-1.6
-1.8
-2.0
-2.2
-2.4
-2.6
-2.8
32.4
33.2
34.0
34.8
35.6
36.4
37.2
38.0
38.8
39.6
40.4
41.2
42.0
42.8
43.6
44.4
45.2
46.0
46.8
$10^{-3} \cdot E_u(K)$, cm^{-1}

Figure 19

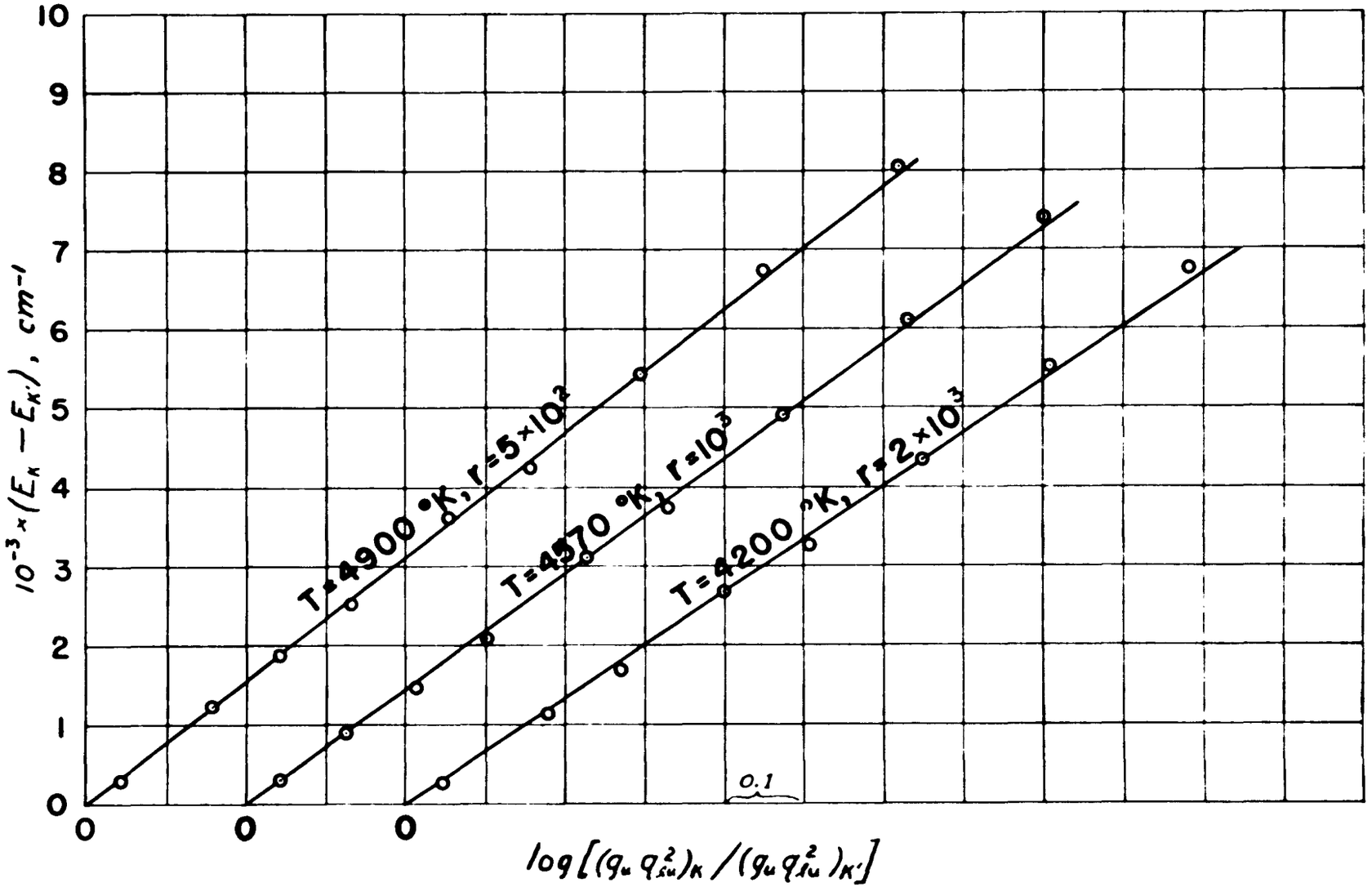
10
9
8
7
6
5
4
3
2
1
0
0
0
0
$10^{-3} \times (E_K - E_{K'})$, cm^{-1}
T=4900 °K, r=5×10²
T=4570 °K, r=10³
T=4200 °K, r=2×10³
0.1
$\log[(q_u q_{lu}^2)_K / (q_u q_{lu}^2)_{K'}]$

Figure 20

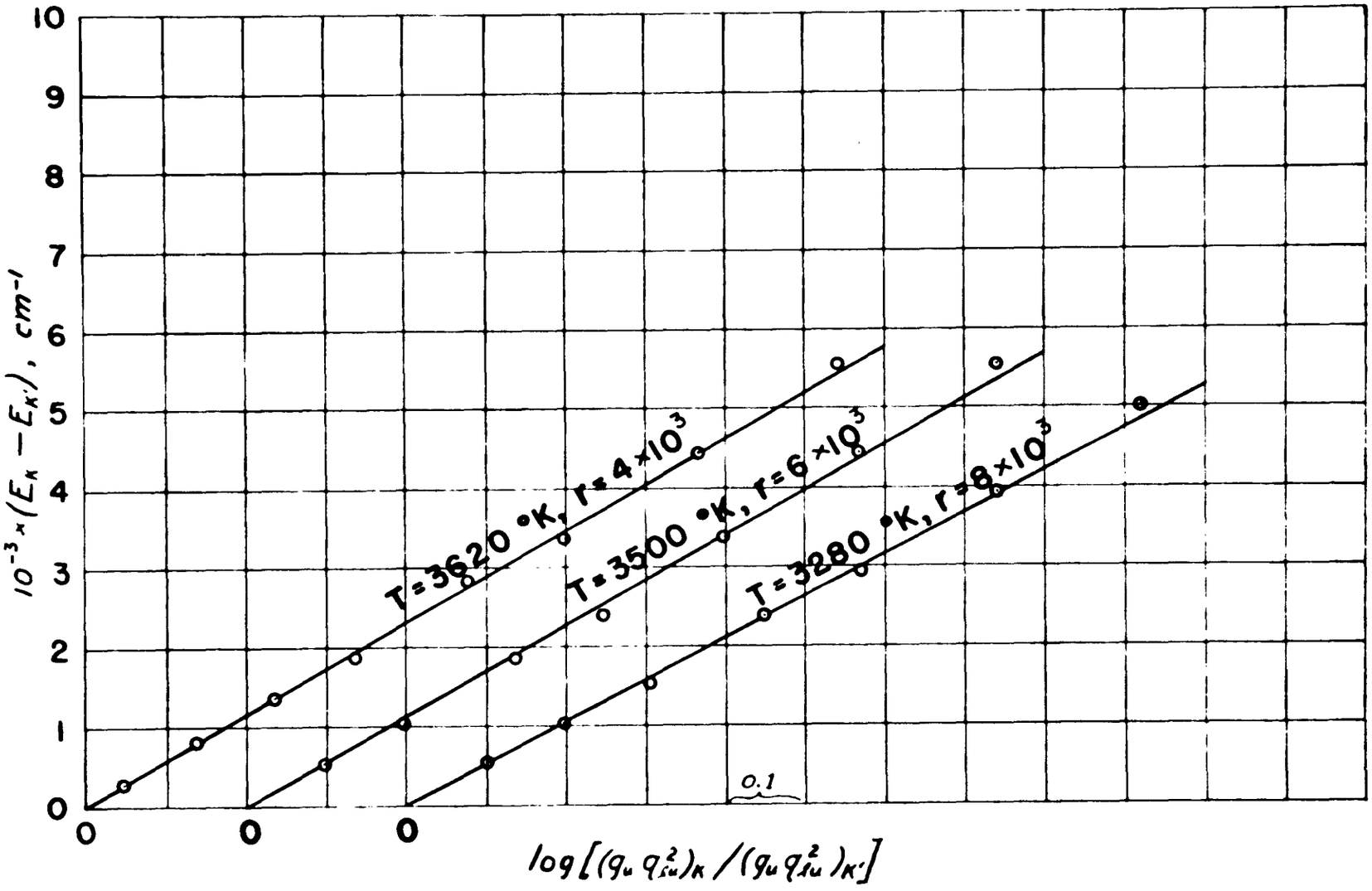
10
9
8
7
6
5
4
3
2
1
0
0
0
0
$10^{-3} \times (E_K - E_{K'})$, cm^{-1}
T = 3620 °K, r = 4×10^3
T = 3500 °K, r = 6×10^3
T = 3280 °K, r = 8×10^3
0.1
$\log[(g_u q_{iu}^2)_K / (g_u q_{iu}^2)_{K'}]$

Figure 21

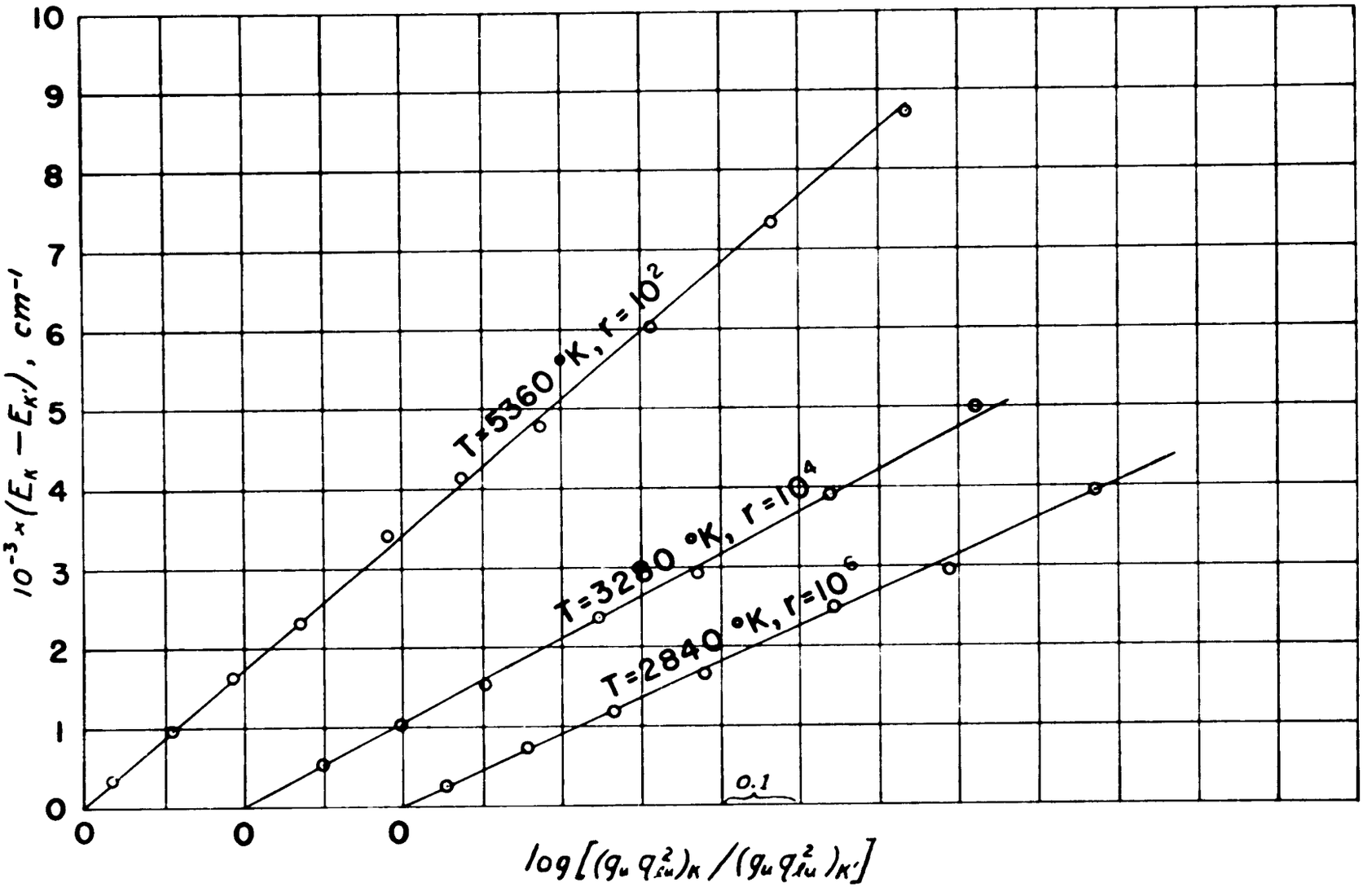
10
9
8
7
6
5
4
3
2
1
0
0
0
0
$10^{-3} \times (E_K - E_{K'})$, cm^{-1}
T=5360 °K, r=10^2
T=3280 °K, r=10^4
T=2840 °K, r=10^6
0.1
$\log[(g_u q_{iu}^2)_K / (g_u q_{iu}^2)_{K'}]$

Figure 22

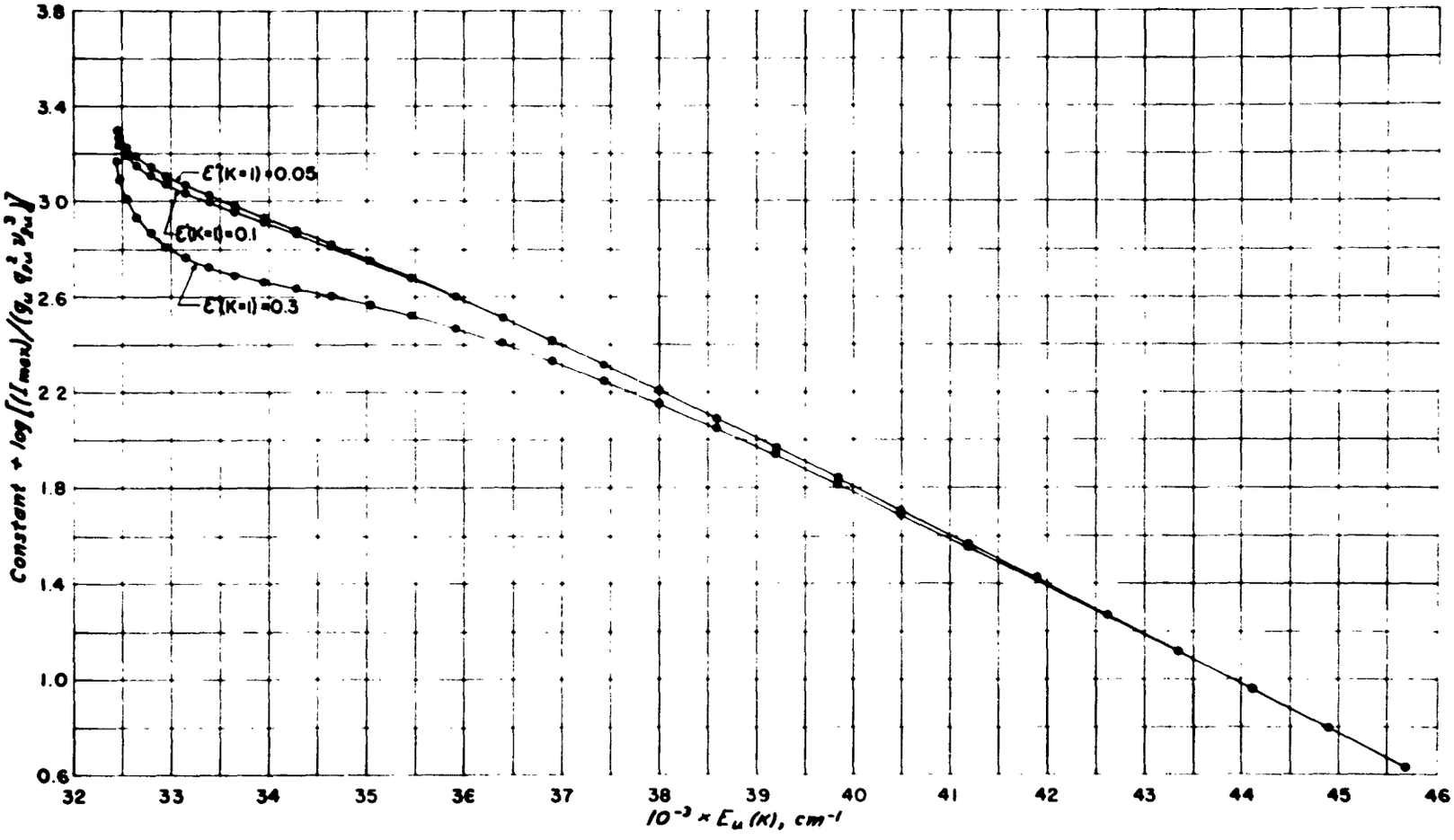
3.8
3.4
3.0
2.6
2.2
1.8
1.4
1.0
0.6
32
33
34
35
36
37
38
39
40
41
42
43
44
45
46
ε(K=1)=0.05
ε(K=1)=0.1
ε(K=1)=0.3
Constant + log[(I_mod)/(g_u q²_mu ν⁴_mu)]
10⁻³ × E_u (K), cm⁻¹

Figure 23

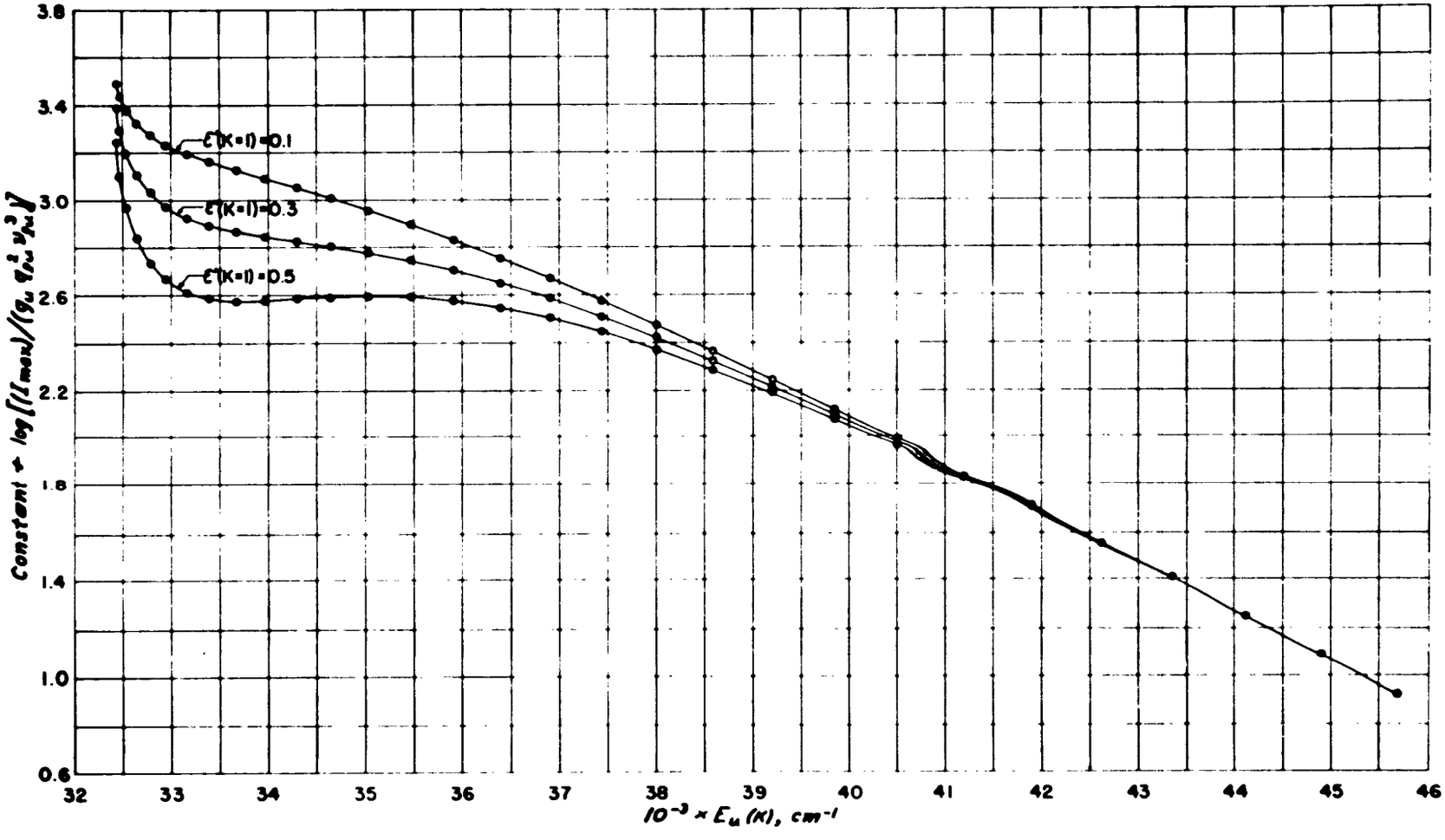
3.8
3.4
3.0
2.6
2.2
1.8
1.4
1.0
0.6
32
33
34
35
36
37
38
39
40
41
42
43
44
45
46
ε'(K=1)=0.1
ε'(K=1)=0.3
ε'(K=1)=0.5
Constant + log[(I_max)/(g_u q²_u v³_u)]
10⁻³ × E_u (K), cm⁻¹

Figure 24

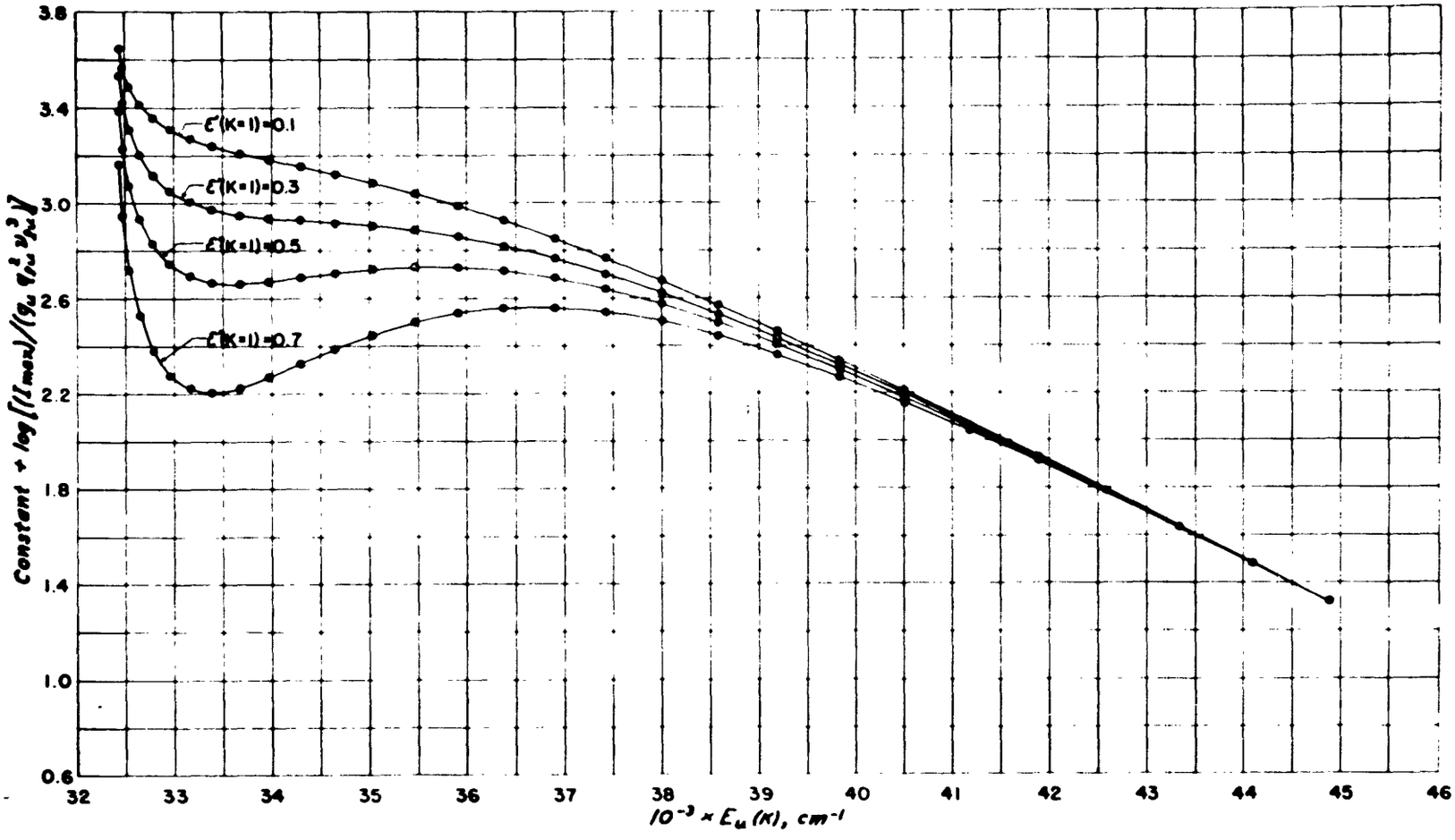
ε'(K=1)=0.1
ε'(K=1)=0.3
ε'(K=1)=0.5
ε'(K=1)=0.7
Constant + log[(I max)/(S_u g_u A_u ν_u^2)]
10^-3 × E_u (K), cm^-1
3.8
3.4
3.0
2.6
2.2
1.8
1.4
1.0
0.6
32
33
34
35
36
37
38
39
40
41
42
43
44
45
46

Figure 25

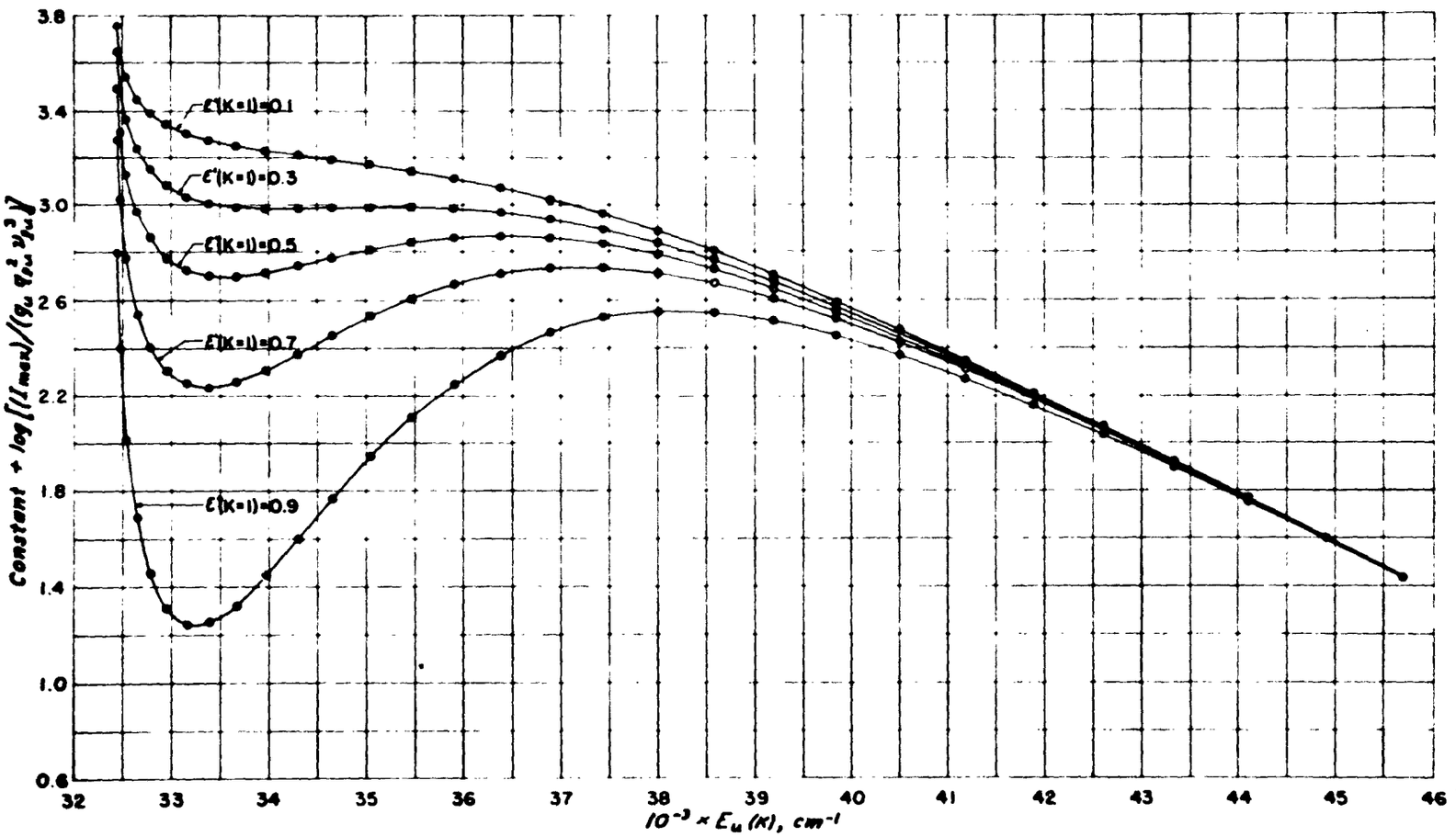
ε'(K=1)=0.1
ε'(K=1)=0.3
ε'(K=1)=0.5
ε'(K=1)=0.7
ε'(K=1)=0.9
Constant + log[(I max)/(g_u q_u² ν_ul²)]
10⁻³ × E_u (K), cm⁻¹
3.8
3.4
3.0
2.6
2.2
1.8
1.4
1.0
0.6
32
33
34
35
36
37
38
39
40
41
42
43
44
45
46